CHAPTER 3

LUNAR OCCULTATION METHOD, OBSERVATIONS AND THE DATA

Lunar Occultation of radio sources is a technique with which one can obtain arcsec resolutions at metre wavelengths, even with a moderate sized antenna and without getting bogged down by the otherwise complicated ionospheric or tropospheric refraction effects. In fact until a few years back the lunar occultation technique was the only way to get the detailed brightness distribution (even if only one-dimensional) with arcsec resolutions at metre wavelengths. It was the accurate radio position of 3C273, determined by its lunar occultation observations with the Parkes 210-foot dish by Hazard et al. (1963), which led to the discovery of first quasar.

A lunar occultation of a radio source is said to take place when the Moon passes between it and the observer. The intersection of the rims of the Moon at the times of disappearance (immersion) and reappearance (emersion) of the source, immediately yield the source position. Moreover the shape of the occultation curve provides information about the strip-scan brightness distribution along a direction perpendicular to the limb of the Moon at the point of occultation. As the strip scans may lie along different position angles for different events, each immersion or emersion separately considered as an event, we also get some knowledge of the two-dimensional brightness distribution across the source from these strip scans. This is more so in the cases where, due to repeat occultations of the same source, we have many scans available across the source along different position angles. Especially in case of 'double' radio sources, where the emission arises largely from two widely separated discrete components straddling the optical galaxy or quasar, the occultation position for each of the two components is determined from 2 or more scans, thus giving us an accurate estimate of the LAS (largest angular size) and PA (position angle) of the major axis of the source. The height of the occultation step also gives the flux density of the source.

3.1 LUNAR OCCULTATION METHOD AND TECHNIQUE

The various details of the occultation technique have already been well documented (see e.g., Hazard 1976; Scheuer 1962; von Hoerner, 1964; Sutton 1966). Accordingly we shall consider only some of the points relevant for the observations described here.

The occultation observations were made using ORT, which tracked the moon continuously in hour angle from $-4^h\ 07^m$ upto $+5^h\ 20^m$. In declination the multiple beam system was exploited to cover the moon. The analogue outputs of 12 beams were recorded on chart-records, while simultaneously the digitized data were also recorded on a magnetic tape using a sampling time interval of 0.5 sec. An effective time constant of 1.0 sec was routinely used for these observations. Normally calibration was done both at the beginning and at the end of the observations. After the daily observations were over, the chart records were examined visually for the presence of any occultation steps. As the record quality was very good, it was normally possible to detect an occultation step of a 0.2 Jy source without any difficulty. From the observed time of a single occultation (i.e. either immersion or emersion) and from the approximate declination of the source, known from the beam position in which occultation took place, time of the other occultation within about a minute of accuracy was calculated. Only those occultations were considered to be genuine, where the second step (immersion or emersion) was found within the expected time range.

Once the occurence of occultations were pin-pointed then the restorations of the one-dimensional brightness distributions were obtained using the deconvolution method, worked out firstly by Scheuer (1962) and subsequently developed by von Hoerner (1964). Depending upon the preliminary estimate of the flux of source, a set of six resolutions, generally within 1 to 30 arcsec, were chosen and for these computer restoration outputs were generated. Then the restored outputs for each source were carefully examined. Starting from the finest resolution, coarser resolutions were scanned till a minimum signal to noise ratio of >4 was obtained for the total source or for the discrete components of the multiple-component sources. A least-square guassian fit was made to each discrete component and from this the peak position, full half-power width and flux under the component were determined, along with estimated errors as described later. The rough estimate of the total flux of the source was made from 30 sec average output of the occultation curve plotted at least for ±15 min about the occultation time. In general the total flux from the various components of a source was found to be the same as that seen on the 30 sec average plot. This counter-check was especially helpful for locating the faint emission extending over region larger than about 30 arcsec, as well as for getting an indication of the weak secondary components due to the missing flux in the sum total of main components. While examining the analogue chart records, particular attention was paid to look for any broad occultations which are likely to be less prominent in the baseline drift caused by Moon's slow motion in north-south through the beams. Also all confirmed occultations were checked for any missed secondary components within about ±10 minutes of the occultation on chart-records in the main beam as well as in adjacent beams on either side.

We discuss below some of the salient points in the determination of

(a) radio position (b) optical identification (c) one-dimensional radio structure and size and (d) flux-density.

3.1.1 Radio Position Determination

The intersection of the Moon's limbs at the precise times of immersion and emersion gives immediately the position of the occulted radio source. The ambiguity of the actual position among the two intersections is easily resolved by knowing the approximate declination of the source from the pointed position of the beam in which occultations took place. The determinations of the occultation timings from the analogue charts were accurate to within about 10 seconds, the fine corrections to these were made from the peak position obtained from the restored outputs. Peak positions and thus the radio positions were determined for all discrete components in the one dimensional restored brightness, as well as for the overall centroid. The fine corrections also included the effects of the irregularities in the projected Moon's limb, these were determined from the Moon's limb profiles given by Watts (1963). The errors in peak positions for the individual scans were estimated basically from the expressions given by von Hoerner (1964); the original expressions which were in terms of the input signal to noise ratio were modified in terms of the actual observed signal to noise radio in the restored outputs. The expression used by us for error in the position determination in an individual scan is $0.56\sigma_0\beta_m/F$, where σ_0 is the measured output noise, β_m is the measured half power width and F is the flux of the radio component. An additional gaussian error of 0.5 arcsec was added to take care of the uncertainties in Watts corrections, time uncertainties, uncertainties in position angles etc. The final error $\sigma_i = \sqrt{[(0.56\sigma_0\beta_m/F)^2 + (0.5)^2]}$, assigned to each particular scan, was used in calculating the final position error.

In many cases more than two scans were available because of the repeat occultations of the same source. In these case the radio position was estimated by minimizing its distance from the Moon's limbs for various scans; while estimating this distance a proper weightage $\omega_i = 1/\sigma_i^2$ was given to each scan. For calculation purposes, each of the Moon's limbs was replaced by a tangent at the contact point. The formulae used are given below (see also von Hoerner, 1966).

Suppose there are n occultation scans for a given source. We choose a co-ordinate system x,y with its origin (0,0) at some suitable point chosen in the vicinity of the final expected position, the choice being otherwise arbitrary. Let d_i be the distance of the Moon's limb from the chosen origin (0,0) in its ith scan along the position angle θ_i, and let ω_i be the weightage factor for this scan. Then the final position coordinates X, Y with respect to the origin (0,0) are given as

$$X = \frac{1}{\Delta} \sum_{i=1}^{n} \omega_i d_i X_i \quad \text{and} \quad Y = \frac{1}{\Delta} \sum_{i=1}^{n} \omega_i d_i Y_i$$

where $X_i = \sum_{j=1}^{n} \omega_j \cos(\theta_j) \sin(\theta_i - \theta_j)$,

$$Y_i = \sum_{j=1}^{n} \omega_j \sin(\theta_j) \sin(\theta_j - \theta_i)$$

and

$$\Delta = \sum_{i=1}^{n} \sum_{j=1}^{n} \omega_i \omega_j \sin(\theta_i) \cos(\theta_j) \sin(\theta_i - \theta_j)$$

$$= \sum_{i=1}^{n} \omega_i \sin(\theta_i) X_i = \sum_{i=1}^{n} \omega_i \cos(\theta_i) Y_i \ .$$

The errors σ_x and σ_y in the final position X and Y are then given by

$$\sigma_x = \frac{1}{\Delta} \sqrt{\left[\sum_{i=1}^{n} \omega_i X_i^2\right]} \ , \quad \sigma_y = \frac{1}{\Delta} \sqrt{\left[\sum_{i=1}^{n} \omega_i Y_i^2\right]} \ .$$

3.1.2 Optical Identification

The radio positions determined from lunar occultation are normally accurate to within a few arcsec. This allows us to check for any optical counterpart of the source with a great amount of certainty. In every case the optical field within a circle of a minute of arc of the radio position was examined on the Palomar Sky Survey (PSS) prints using a transparent overlay. Optical positions of 2 or 3 nearest objects to the radio position, but lying within the circle, were measured on negative contact prints made from PSS prints using the X-Y co-ordinate measuring machine. Their right ascensions and declinations were determined from similar X-Y measurement of 8 or more SAO reference stars more or less uniformly distributed within a degree around the source position. The optical positions thus obtained are generally believed to be accurate to ±0.5 arcsec in both co-ordinates. In case of some very faint optical objects, whose direct image was not visible on negative contact prints, a secondary set of 3 or more nearby optical objects was used to calculate the position of the faint object. In such cases the rms error in each co-ordinate may be as large as ±2 arcsec. Optical magnitudes have been estimated using the procedure given by King and Raff (1977). The magnitude estimates are accurate to within ±0.5 mag for stellar objects, but this uncertainty may be somewhat larger for the galaxy type objects.

3.1.3 Angular Size Determination:

Whenever a source appeared to have a resolved structure we have also attempted to quantify the error estimation in size. The formulation is based on that given by von Hoerner (1965). As mentioned earlier a
fit was made to each discrete component giving its half-power wi

and flux along with the peak position. Let β_m be the measured HPW and F be the flux. If σ_0 is the noise in the restored output, then

$$\Delta\beta_m = 1.4\ \beta_m\ \sigma_0/F.$$

Let us define $A = \beta_m^2 - \beta_e^2 - \Delta\beta_m^2$ and $\Delta A = 2\beta_m\ \Delta\beta_m$,

where β_e is the gaussian resolution used. Then angular size, ϕ, is calculated as

$$\phi = \sqrt{A} \pm (\sqrt{A} - \sqrt{(A-\Delta A)}) \quad \text{for } A > \Delta A$$

$$\phi \leq \sqrt{(A+\Delta A)} \quad \text{for } 0 < A \leq \Delta A$$

$$\phi \leq \sqrt{(\Delta A)} \quad \text{for } A \leq 0\ .$$

3.1.4 Flux Determination

As mentioned earlier calibrations were usually done both at the beginning and at the end of the observations. The flux at 327 MHz for the calibrating sources has been adopted from the spectral plots of Veron et al.(1974). As the occulted source may not be lying exactly at the centre of beam (see fig.2.1) its response in all neighbouring beams was used to pinpoint the position of the source within the main beam and accordingly a correction to its flux value was made. For this purpose a computer program was used which convolves the calculated beam pattern (shown in fig.3.1) with the observed relative response of a source in various neighbouring beams. Then the occurrence of a maxima in the convolved output gives us the displacement of the source position from the centre of main beam. Our estimate is that the rms error in flux determination is 15% or 0.1 Jy whichever is larger.

3.2 RADIO AND OPTICAL DATA ON OCCULTATION SOURCES

In this section we present the occultation data on 305 radio sources, observed with the ORT. The data include accurate radio positions,

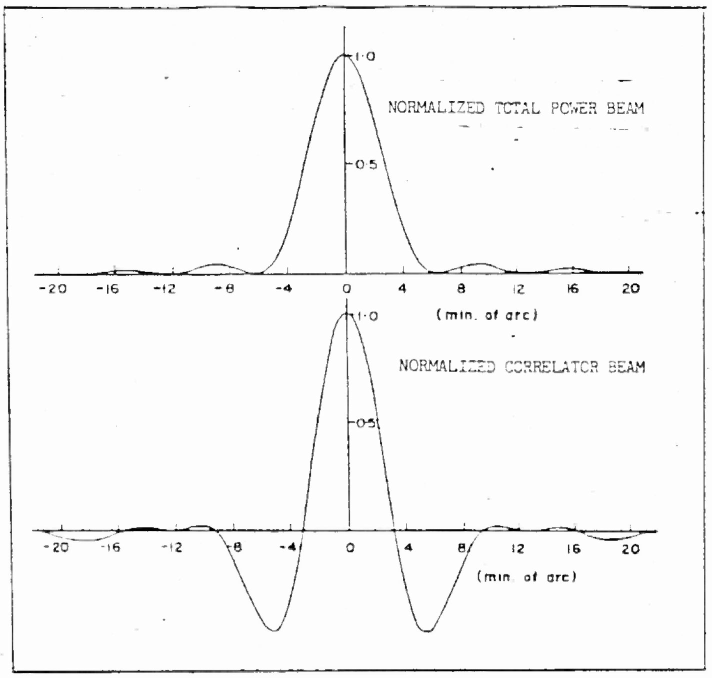

Fig 3.1 Normalized power pattern for the ORT beams

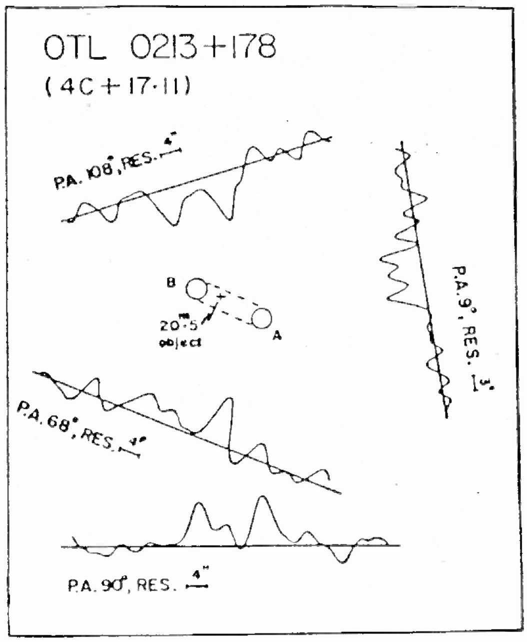

Fig 3.2 Derived radio structure of 0213+178

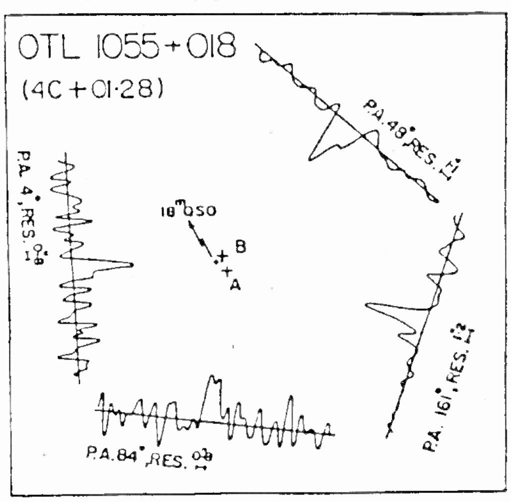

Fig 3.3 Derived radio structure of 1055+018

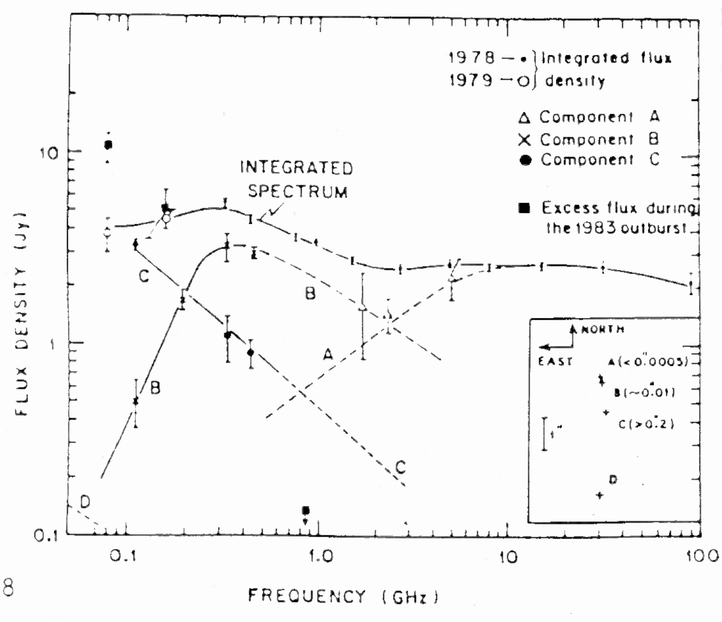

Fig 3.4 Radio spectrum of 1055+018

structural information mainly along two different position angles, the flux density at 327 MHz, and the information about optical identifications. The data is arranged in 2 different tables covering different periods of observations. The finding charts for the newly identified radio sources immediately follow each table. Additional structural notes for some of the sources in the two table are given below.

3.2.1 Additional Structural Notes For Sources In Table 3.1

0213+178 : This double source (fig.3.2) shows a continuous bridge of emission accounting for about 15 percent of the total flux. But this emission could even be arising from a central component coinciding with the optical object (Table 3.1).

0418+236 : The head lies towards the northern edge of an extended feature which has a length of about 0.5 arcmin in PA 45° and a transverse width less than 6 arcsec.

0459+246 : About 4 arcmin away from this source, along a position angle of 60°, a weak source of about 0.4 Jy (size < 8 arcsec in PA 140°) lies. These two sources donot appear to be connected by a detectable bridge of emission, but an 18 mag NSO is seen approximately midway between the two.

0521+238 : The unresolved core (Table 3.1) is superimposed on a possible halo of size about 0.5 arcmin containing about 10 to 20 percent of the total flux.

1039+029 : About 30% of the total emission arises from a central component or a bridge.

1052+016 : The source has a head-tail structure and lies just outside the boundary of the Abell cluster, A 1139 (Abell 1958). The tail accounts for about half of the total flux at 327 MHz and extends by about 15 arcsec along PA 70°, thus pointing towards the centre of A 1139.

1055+018 : The present observations show the source is double (fig. 3.3, Table 3.1) with the stronger component B coinciding with the 18 mag QSO. Gopal-Krishna et al. (1984) have derived the detailed structure of this QSO by using our occultation structure, IPS observations at 327 MHz and various VLBI data, available in the literature. The quiescent radio structure from these data and from the available detailed spectral information (fig. 3.4) appears to consist of four components, two of which are rather compact (see inset in fig.3.4 for a schematic diagram). Recently Slee (1984) has observed large flux variability at 80 MHz and 160 MHz in this source, a detailed analysis of which is given by Gopal-Krishna et al.(1984).

1148-050 : At 327 MHz, the source consists of a core (size<3 arcsec in PA 0°) connected to the 19 mag galaxy (Table 3.1) by an extended radio feature of similar intensity. About 2 arcmin southeast of this source is seen a weak source of about 0.3 Jy.

1237-101 : The source is a flat spectrum quasar with z=0.753 (Wills & Wills 1976). At 327 MHz it has a weak extension of about 5 arcsec towards west. The optical position (Table 3.1) is taken from Hunstead (1971).

1531-221 : This source lies only 6 arcmin away from OTL 1531-220 (Table 3.1). Neither a bridge of emission at 327 MHz nor any peculiar optical object is observed in between the two sources.

1618-235 : The stronger component A shows a sharp outer edge and an extension towards component B. Bolton et al. (1975) have identified the source with a 16.5 mag E-galaxy, which is not confirmed by the present observations.

2059-135 : The Molonglo map at 408 MHz shows the source to be an equal double with the 15.5 mag E-galaxy (z=0.0296, member of a loose cluster) lying in the centre (Schilizzi and McAdam 1975; Schilizzi 1975). The present observations with a higher resolution indicate a central radio component of a size smaller than 40 arcsec in PA 53° which accounts for about 20 per cent of the total flux and is likely to be associated with the E-galaxy. The optical position (Table 3.1) is from Schilizzi (1975).

2243-032 : The core described in Table 3.1 accounts for about 60 percent of the total flux at 327 MHz while the remaining flux arises from a south-westerly extension of about 5 arcsec.

2303-008 : Alternate possible positions for components would imply a component separation of about 10 arcsec in PA ~65°.

2338+030 : The source has been identified with a 19 mag E3 galaxy (McEwan et al. 1975) elongated in the north-south direction. The dominent core, whose size is given in Table 3.1, accounts for about 80 percent of the total flux and can be identified with the scintillating component of size <0.5 arcsec observed at 318 MHz by Harris (1973). The remaining flux originates in two jets of size about 5 arcsec each, extending east and west from the core.

3.2.2 Additional Structural Notes For Sources In Table 3.2

0016+054 : A possible component with a flux density of ~0.15 Jy lies at ~10 arcsec along PA~235°.

0054+078.1 & 0054+078.2 : The Ohio source OB 091 (Fitch et al.1969) appears to be a blend of these two sources. We have not detected any bridge of emission connecting the two sources. The soucrce 0054+078.2 has about 25% of its total flux arising from a western extension of about 1 arcmin.

0054+090 : Component A consists of two subcomponents of equal flux density at 327 MHz. The remaining flux is in component B of size <3 arcsec and lying at 16 arcsec from component A in PA ~35°.

0153+136 : The source is a clear equal double with component separation of 25 arcsec. Because of ambiguity in pairing, it is not possible to give a unique value for the position angle of separation. The two possible value are 90° or 150°, the latter value being in agreement with the model given by Cotton et al.(1975).

0156+126 : The western component B in itself is an equal double.

0156+136 : A possible halo of size ~ 8 arcsec containing ~20% of total flux.

0200+130 : The source is a clear double with east-west separation of about 36 arcsec. North-south separation is not known as there was heavy interference during the occultation along that position angle. The western and weaker component could itself be an equal double, while the eastern component has a core of size <4 arcsec surrounded by an equally strong diffuse feature of about 20 arcsec in size.

0232+150 : About 20% of the total flux is contained in a diffuse extension of size ~30 arcsec along PA ~65°.

0255+173 : The source is possibly double with east-west separation of about 25 arcsec.

0312+180 : About one-third of the total flux (Table 3.2) arises from a diffuse east-west component of about 1 arcmin size around the compact component.

0325+179 & 0325+180 : 0325+179 is within 4 arcmin of 0325+180. There is neither any detectable bridge of radio emission between the two nor any peculiar optical object is seen on the line joining these two sources. Moreover, 0325+179 is itself identified with a blue galaxy. Therefore, these two radio sources are unlikely to be physically connected. Large errors or limits in Table 3.2 are due to the presence of interference by thunder storms. There could be another source of flux density of 0.6 Jy a few arcmin west of 0325+180.

0329+175 : About one-third of the total flux arises from a 30 arcsec long diffuse component, which is elongated in PA~140°.

0343+184:About 40% flux of component B is contained in a diffuse feature of size ~30 arcsec.

0359+193 : The source, which lies in an open Zwicky cluster 0357.2+1850 (Zwicky et al. 1965), could be having a head-tail structure with about two-thirds of the total flux in the tail,extending upto about 90 arcsec along PA ~85°. A 16 mag galaxy, which is the brightest member of the cluster, lies 32.5 arcsec south-east of component A.

0436+203 : The source seems to have a triple structure with equal flux in each of the three components with the outer components symmetrically placed around the central one which coincides with the centroid.

0455+201 : The source has a western extension of ~ 15 arcsec containing about 20% of the total flux. There is a 17 mag NSO lying at the western end of this extension.

0519+196 : There is a possible second component containing about 20% of the total flux and lying at about 4 arcsec east of the main component. The 18 QSO earlier identified by Wills and Bolton (1969) lies about 80 arcsec north of the occultation position.

0529+198 : Pairing of components in the two occultation scans is ambiguous. The alternate pairing gives a separatioin of about 11.5 arcsec along PA~5°.

0539+198 : It is a clear equal double source with east-west separation of about 20 arcsec. The north-south separation of ≥60 arcsec is estimated from the relative response of the individual components among neighbouring beams of the telescope.

0628+191 : If interpreted as a head-tail source, the head has a size of ~25 arcsec and contains about 75% of total flux and the tail extends upto ~80 arcsec along PA ~25°.

0708+184 : Component B is more extended. There are a number of faint red objects in the background field. Because of crowded field, the identification may not be reliable.

0806+152 : The stronger component A itself could be an equal double. About 10% of the total flux may be in bridge connecting the two components.

0925+092 : This source consists of two components, one of which is compact with a size of <2 arcsec, the other being diffuse extending upto ~15 arcsec towards south from the compact component. The two components are roughly equal in intensity.

0946+076 : Component A has a diffuse feature of extension ~35 arcsec towards component B which contains about 20% of the total flux. It is interesting to note that a 19 mag BSO lies only 10 arcsec away from the identified galaxy.

0949+077 : Willis et al.(1976) have found that it is an equal double source with a component separation of 49 arcsec along PA 112°, which is consistent with the occultation results. The 20 mag red galaxy (Table 3.2) lies within 6 arcsec of the position of the western radio component given by Willis et al.

1033+038 : The source is possibly double with the weaker and diffuse component lying along PA ~234° from the main component.

1039+035 : The source could be having a head-tail structure with the tail accounting for two-thirds of the total flux and extending from the compact component A to about 50 arcsec along PA 60°.

1048+022 : There could be a secondary component with a flux density of 0.1 Jy lying at about 90 arcsec south of the main source.

1201-041 : The optical field lies in a cluster of galaxies. The radio source consists of three components. There are three galaxies in the radio region. Table 3.2 lists the galaxy nearest to the radio axis which we have suggested as the optical identification.

1220-059 : The component A is itself an equal double.

1348-129 : About 15% of the total flux is accounted for by an extension of about 5 arcsec in PA~150°. The finite size along PA~75° given in Table 3.2 may be due to this extension.

1416-156 : There is another 20 mag galaxy about 10 arcsec south of the position given in Table 3.2. The source possibly has three components, but it is not possible to determine accurately their individual positions.

1452-168 : There could be a secondary component of flux density of 0.25 Jy at 50 arcsec away from the main component along PA~75°.

1456-165 : There could be a secondary component of flux density of 0.2 Jy 30 arcsec north-east of the main component.

1628-211 : About 20% of the total flux could be arising from a south-westerly extension of about 5 arcsec.

1655-201 : About 50% of the total flux is in diffuse features, which extend upto about 30 arcsec towards south of component A. The identified galaxy coincides with component A.

1723-203 : A secondary component of 0.1 Jy lies at about 60 arcsec from the main component along PA~135°.

1918-185 : About one-third of the total flux is in a diffuse feature which extends upto about 20 arcsec along PA 215°.

1922-183 : 25% of the total flux could be in a western extension of about 15 arcsec.

2120-102 : There could be a diffuse feature of 2 arcsec extent around the compact source and accounting for about 10% of the total flux.

2322+011 : There seems to be a diffuse component containing ~20% of the total flux and extending to about 90 arcsec in south-west direction of the main component.

2342+023: The eastern component A is itself an equal double with a component separation of 10 arcsec.

3.2.3 Tabulated Data

The derived radio and optical parameters for each source are given in Tables 3.1 and 3.2. The entries in the Tables are arranged as follows:

Column 1 : The source name with the prefix OTL. An astrisk(*) preceding the name implies that additional notes and comments are given in the text.

Column 2 : Total number of occultations used in deriving the various tabulated information for that source. A single immersion or emersion is called an occultation.

Column 3 : Name of the individual component of a source, if not single. The components are named A,B,C in order of increasing right ascension. The symbol 'S' in this column implies that the multiple component structure of this resolved source appears merged along that scan angle, and that the tabulated angular size information along that position angle is for the whole source, treated as a single component.

Column 4 : Flux density S_{327} for the whole source or for an individual component.

Column 5 : Position angle of scan (PA).

Column 6 : The effective resolution achieved (β_e).

Column 7 : The derived angular size information for the whole source or for the individual component along the PA mentioned in Column 5.

Columns 8,9,10 : Similar to Columns 5,6,7 respectively, but corresponding to another available scan.

Columns 11,12 : Overall structure of the source. The largest angular size (LAS) is entered in Column 11 and the position angle of the major axis of the source is given in Column 12.

Column 13 : Abbreviated notes to the overall morphology of the source. The following abbreviations are used :

U, unresolved; S, single; D, double; PD, possibly double; PD : , possible double with flux ratio of the western to the eastern component; HT, head-tail; Extn, a weak extension in addition to the tabulated component; CH, core-halo; T, triple; Br%, bridge with the percentage of flux in the bridge; Cx, a more complex structure than the above mentioned classes. A question mark (?) implies that the tabulated morphology class is not very certain.

Columns 14,15,16 : The radio position information, right ascension (RA) and declination (Dec), in the 1950.0 epoch is given in Columns 15 and 16 along with the standard errors. 'CN' in Column 14 indicates centroid position. The symbol 'a' under position errors implies that the errors are better specified along two mutually perpendicular position angles given in the foot-notes to the Table. Such a case arises whenever all the available position angles of scan for a source are seperated only by a small angle.

Columns 17,18 : The radio minus optical position difference for the optical object entered in the Column 20. The optical positions are generally accurate to ~0.5 arcsec. But when the position differences are enclosed in parentheses, they imply an uncertainty of ±2 arcsec in optical position for the corresponding optical object.

Column 19 : Photographic magnitude of the optical object, estimated visually from the blue (O) PSS prints. The estimates are based on the scale given by King and Raff (1977) and may be uncertain by ±1 magnitude.

Column 20 : Abbreviated notes on optical objects. A dagger (†) indicates a positive or likely identification. References to earlier published finding charts are given by coded numbers in parentheses, and these codes are explained in the foot-notes. The following abbreviations are used for the notes on optical objects :

EF, empty field; Cwd, crowded field; Obsc, obscured field; INP, identification not possible because of either large errors in radio position or because of the presence of more than one optical object within the error box; QSO, quasi-stellar object; BSO, blue stellar object; RSO, red stellar object; NSO, neutral stellar object; G, galaxy; EG, elliptical galaxy; BG, blue galaxy; RG, red galaxy; BO, blue object; RO, red object; NO, neutral colour object; Cl, cluster. A question mark (?) indicates that the given optical class is not very certain.

Column 21 : Galactic lattitude $|b^{II}|$ of the source.

Column 22 : Other catalogue names, generally only the better known ones are given.

The finding charts for 66 newly identified objects are given in Plate 3.1 and Plate 3.2.

Table 3.1 Occultation data on 65 radio sources.

(1) Ooty name (OTL)	(2) No. of occ.	(3) Comp	(4) Flux den. Jy	(5) PA deg	(6) βe "	(7) Angular size "	(8) PA deg	(9) βe "	(10) Angular size "	(11) Overall Source Structure: LAS "	(12) PA deg	(13) Notes	(14) Comp	(15) Radio position (1950.0) RA h	m	s	(16) Dec °	'	"	(17) Rad-Opt ΔRA "	(18) ΔDec "	(19) Optical object m_{pg}	(20) Notes	(21) b^{II} deg	(22) Other Catalogue names
0042+101	2		1.0							50	141	D	CN	00	42	22.80±0.40	+10	10	31.5±6.0	+1.0	+2.0	18	† QSO	52	MC2
		A	0.7	14	15	<15	119	30	≤22				A	00	42	22.07±0.27	+10	10	45.3±2.0						
		B	0.3	14	30	<30	119	30	≤30				B	00	42	24.20±0.40	+10	10	06.0±6.0						
0058+113	2		0.6	43	8.1	≤6.5	68	8.1	≤6.5			U		00	58	51.23±0.25	+11	19	19.5±4.0	(-3	+1)	20	† BSO ?	51	OB+197
0130+142	2		1.0	55	8.0	7.0 ±5.0	69	8.0	≤10			S		01	30	44.80±0.30	+14	14	27.0±5.5				EF	47	OC+151
0135+147	4		0.6	20	15	≤14	63	15	≤11			U		01	35	29.25±0.11	+14	46	38.3±1.9				EF	46	
				95	20	≤22																			
0140+157	3		0.5	35	15	≤11	57	4.2	≤5.0			U		01	40	32.60±0.12	+15	42	34.1±2.4				EF	45	
				110	30	≤25																			
0147+160	2		0.9	40	15	15 ±12	99	15	18.0±5.0			S		01	47	54.20±0.15	+16	05	40.0±2.5				EF	44	MC3
0157+168	2		0.7	52	30	21 ±12	67	20	21 ±15			S		01	57	46.45±a	+16	49	06.0±a				EF	43	MC3
0206+168	2		1.6	49	2.2	≤2.5	81	8.1	18.5±3.5			S		02	06	58.08±0.11	+16	48	52.2±2.1				EF	42	4C+16.05
*0213+178	6		3.0							14.4	66	Br 15%	CN	02	13	46.53±0.03	+17	52	40.7±0.6	(-3	-1)	20.5	†BG?(11)	40	4C+17.11
		A	1.5	9	3.1	≤3.0	108	4.1	≤2.5				A	02	13	46.15±0.02	+17	52	37.2±0.5						
		B	1.0	9	3.1	≤3.0	88	4.2	≤3.0				B	02	13	47.07±0.03	+17	52	43.0±1.0						
0214+183	2		1.1	32	20	≤20	89	20	≤17			U		02	14	39.61±0.11	+18	23	07.5±2.5				EF	40	H
0229+185	2		0.5	38	31	≤37	87	31	≤22			U		02	29	38.00±0.30	+18	34	23.0±10				C1?	38	OD+149
0302+206	2		0.9	42	15	19.5 ±8.5	89	8.2	≤7.5			PD, 1 : 1		03	02	14.89±0.10	+20	39	13.5±3.0				EF	32	OE+202
0304+206	2		0.4	33	31	55 ±15	98	31	37 ±17			S		03	04	52.28±0.30	+20	39	00.0±5.0	−15.9	+7.9	19	†RSO	32	
0312+212	2		0.3	63	31	≤35	104	41	60 ±30			S		03	12	57.50±0.40	+21	16	35.0±12	+3.6	+31.4	19.5	BG?	30	
0315+214	2		1.0	74	10	15.0 ±5.0	99	8.2	13.0±7.0			PD, 1 : 1		03	15	38.47±0.10	+21	29	49.8±6.0				EF	30	OE+226
0322+213	2		1.5	52	8.1	6.9 ±1.6	105	3.1	≤3.0			PD		03	22	32.92±0.07	+21	19	31.6±1.0				EF	29	4C+21.11
0334+220	4		2.0							52	83	D	CN	03	34	29.10±0.20	+22	01	01.0±3.0	−16.3	+9.9	18.5	RG ? (6)	26	4C+21.12
		A	1.3	43	10	7.5 ±5.0	95	8.1	7.5±4.5				A	03	34	27.85±0.07	+22	00	58.8±1.5						
		B	0.7	43	15	≤15	95	30	≤30				B	03	34	31.59±0.20	+22	01	05.4±4.0						
0412+236	4		1.0							25.5	105	D	CN	04	12	11.61±0.12	+23	40	19.9±0.8					19	B2.4
		A	0.3	14	8.3	≤15	142	8.3	≤15				A	04	12	10.50±0.35	+23	40	25.4±4.0	−4.4	+2.7	20	† G ?		
		B	0.7	14	4.2	≤2.5	142	4.2	≤3.0				B	04	12	12.29±0.10	+23	40	18.8±1.0	+1.4	+4.1	20	† RG ?		
0413+236	2		0.3	49	8.3	≤6.0	112	8.3	≤7.0			U		04	13	18.18±0.10	+23	36	35.0±2.0	−4.7	−2.7	20.5	† RO	19	
*0418+236	2		2.1									HT	CN	04	18	21.18±0.10	+23	41	58.0±1.5	+2.2	+1.1	20	† RSO,Def?	18	4C+23.08
		H	1.4	53	2.2	≤2.5	132	2.2	≤2.0				H	04	18	21.36±0.07	+23	42	00.7±1.0						

(1)	(2)	(3)	(4)	(5)	(6)	(7)	(8)	(9)	(10)	(11)	(12)	(13)	(14)	(15)	(16)	(17)	(18)	(19)	(20)	(21)	(22)
0425+234	2		2.2	61	3.1	2.4 ±1.5	128	15	≤10			S		04 25 57.91 ±0.20	+23 25 09.8 ±3.0				Obs	17	4C+23.09
*0459+246	2		1.1	30	6.1	≤7.5	133	2.1	≤2.5			U		04 59 12.55 ±0.15	+24 36 40.7 ±1.7				EF	10	B2.2
0503+244	2		0.4	95	4.1	≤4.0						U		05 03 30.10 ±0.30	+24 26 00 ±45				Cwd	10	B2.2
0514+237	4		3.0	30	4.2	3.5 ±1.0	54	4.2	5.0 ±1.5			PD		05 14 38.30 ±0.04	+23 47 59.8 ±0.6				EF	8	4C+23.14
				108	4.3	2.7 ±1.3	145	2.2	≤1.6												
0517+239	4		1.4	70	4.2	≤3.0	109	4.2	≤4.0			U		05 17 30.36 ±0.05	+23 57 08.7 ±1.5				EF	7	
*0521+238	4		2.0	54	2.2	≤1.5	132	2.2	≤2.5			CH?		05 21 02.16 ±0.04	+23 52 25.0 ±1.0				EF	7	PKS
0609+228	2		2.3	51	15	15.5 ±8.5	157	15	17.5 ±9.0			S		06 09 49.70 ±0.16	+22 53 17.3 ±2.0				EF	2	4C+22.13
*0612+227	2		2.4	53	4.1	6.5 ±3.0	163	4.1	≤4.0			S		06 12 33.03 ±0.07	+22 42 45.9 ±1.0				Obs	3	4C+22.14
0628+226	2		0.9	74	10	15 ±5.0	136	10	11.0 ±4.5			PD		06 28 11.76 ±0.15	+22 36 49.9 ±2.5				Cwd	6	B2.4
0656+213	6		2.4	68	1.3	≤0.7	150	1.3	1.5 ±1.0			S		06 56 38.82 ±0.02	+21 21 53.8 ±0.3	—0.6	+0.3	19	†G(4)	11	4C+21.22
0715+202	2		2.2	60	2.2	≤1.6	171	4.1	≤4.0			U		07 15 13.58 ±0.07	+20 15 31.6 ±0.8				EF	15	PKS
0717+195	2		2.0	55	4.2	≤3.0	171	4.2	≤3.7			U		07 17 37.01 ±0.07	+19 30 23.3 ±1.0	+0.4	—1.7	18	†NSO	15	4C+19.28
0747+191	2		0.5	95	15	≤14	112	31	≤30			U		07 47 38.88 ±0.22	+19 09 10 ±21	—25.2	—10.5	20	BSO	21	OI+179.2
0752+185	2		1.8	79	1.4	≤1.0	158	1.4	≤1.4			U		07 52 51.21 ±0.07	+18 31 43.7 ±1.0	—11.4	—3.3	17	NSO	22	4C+18.23
0914+114	6		1.8	86	2.1	≤1.9	122	2.0	≤1.1			U, IPS		09 14 33.86 ±0.03	+11 26 13.4 ±0.6				EF	37	PKS
0925+112	2		0.7	88	20	35 ±12	147	15	14.5 ±6.5			S		09 25 02.50 ±0.20	+11 13 32.3 ±3.0				EF	40	
0926+117	2	S	2.4	70	6.2	7.0 ±2.0	157	6.2	7.0 ±1.5			D	CN	09 26 01.18 ±0.13	+11 47 33.2 ±1.0	+0.5	0.0	19	†QSO(5)	40	4C+11.32
1016+058	5		1.1	78	2.0	1.7 ±1.6	159	1.1	≤0.8			S		10 16 56.80 ±0.04	+05 49 40.1 ±0.6				EF	48	4C+05.41
*1039+029	5		7.2							5.7	17	T or Br	CN	10 39 04.10 ±0.03	+02 58 13.7 ±0.5				EF	51	4C+03.18, MSH10+07
		A	3.5	42	1.2	1.2 ±0.3	127	1.2	≤0.9				A	10 39 04.05 ±0.03	+02 58 12.3 ±0.5						
		B	1.5	42	1.2	≤1.5	127	1.2	≤1.0				B	10 39 04.16 ±0.04	+02 58 17.8 ±0.5						
*1052+023	4	S	1.9	168	2.3	≤2.0				27.6	88	D	CN	10 52 42.96 ±0.10	+02 21 45.8 ±1.5	+1.5	+1.5	17	†PAIR	NSO53	4C+02.31
		A	0.8	95	4.1	6.5 ±2.0	136	6.1	8.5 ±2.0				A	10 52 41.78 ±0.07	+02 21 43.9 ±1.5						
		B	1.1	95	8.1	14.0 ±2.5	136	3.1	5.0 ±1.5				B	10 52 43.61 ±0.10	+02 21 45.1 ±1.5						
*1052+016	4		1.4									HT	CN	10 52 50.34 ±0.07	+01 39 48.3 ±1.0				EF	52	
		H	0.7	52	4.5	5.0 ±2.0	136	2.1	≤3.0				H	10 52 50.19 ±0.04	+01 39 47.5 ±0.6						
*1055+018	8	S	4.0	84	0.8	1.2 ±0.6				1.5	18	D	CN	10 55 55.28 ±0.04	+01 50 03.8 ±0.4	—0.8	+0.4	18	†QSO(2)	53	4C+01.28,
		A	1.0	4	0.8	≤1.0	161	1.2	≤1.0				A	10 55 55.26 ±0.04	+01 50 02.6 ±0.6						
		B	3.0	4	0.8	≤0.8	161	1.2	≤1.0				B	10 55 55.29 ±0.03	+01 50 04.0 ±0.4						MSH10+01[illegible]
1133—032	4		1.4	86	4.2	5.5 ±1.0	118	8.1	20.0 ±4.0			S		11 33 28.12 ±0.04	—03 12 38.4 ±1.2				EF	54	4C—03.44
				169	15	38.0 ±5.0															
*1148—050	3		0.8	1	6.2	10.0 ±2.0	130	30	30 ± 15			Cx ?		11 48 37.40 ± 0.20	—05 01 31.2 ±1.5	—27.2	+3.9	19	†G	54	4C—04.38

(1)	(2)	(3)	(4)	(5)	(6)	(7)	(8)	(9)	(10)	(11)	(12)	(13)	(14)	(15)	(16)	(17)	(18)	(19)	(20)	(21)	(22)
1150—044	4		2.1							24	66	D	CN	11 50 33.00 ± 0.20	—04 26 15.0 ± 3.0	—1.8	+0.6	19	†BG,CI?	55	4C—04.39
		A	0.7	147	2.2	≤ 2.0							A	11 50 31.95 ± 0.25	—04 26 22.0 ± 3.0						
		B	1.4	104	4.2	≤ 3.5	147	2.2	≤ 1.8				B	11 50 33.40 ± 0.10	—04 26 12.3 ± 1.5						
1159—060	4		1.9	92	4.1	≤ 3.7	111	2.2	≤ 2.0			S		11 59 06.55 ± 0.04	—06 00 50.3 ± 1.1	—3.0	+11.3	17	BSO	55	4C—05.48
				122	1.3	1.6 ± 0.5	141	8.1	≤ 4.8												
*1237—101	2		1.8	110	3.2	≤ 3.0	133	2.4	≤ 1.8			U		12 37 07.44 ± 0.08	—10 06 58.6 ± 1.7	+2.8	+2.4	18	†QSO(1)	52	PKS
1248—108	4		0.8	83	8.0	7.0 ± 4.0	168	4.0	≤ 4.0			S		12 48 03.56 ± 0.07	—10 49 16.0 ± 1.0				EF	52	
1432—191	2		0.9	103	15	≤ 13	132	8.0	≤ 6.5			U		14 32 58.80 ± 0.20	—19 10 25.6 ± 3.5				EF	37	OQ—157
1531—220	2		1.0	49	30	35 ± 15	139	20	≤ 21			S		15 31 15.02 ± 0.20	—22 05 34.9 ± 3.0				EF	27	MC1
*1531—221	2		1.0	54	7.9	≤ 6.0	132	15	≤ 8.5			U		15 31 39.70 ± 0.20	—22 07 02.1 ± 3.0				Cwd	27	OR—252
1545—234	2		1.0	55	7.9	9.5 ± 3.0	122	7.9	8.0 ± 2.5			S		15 45 19.44 ± 0.10	—23 27 51.0 ± 2.0				EF	24	OR—275
*1618—235	2		3.3							38.5	72	D	CN	16 18 00.07 ± 0.07	—23 34 55.7 ± 2.1				Obs	18	OS—230,
		A	2.0	91	7.8	9.5 ± 2.0	125	7.8	9.0 ± 2.0				A	16 17 59.07 ± 0.07	—23 35 00.2 ± 1.7						MSH16—203
		B	1.3	91	15	11.0 ± 6.0	125	15	20.0 ± 6.0				B	16 18 01.72 ± 0.10	—23 34 48.0 ± 3.1						
1841—222	2		1.2	50	4.0	≤ 3.0	97	15	≤ 14			U		18 41 43.20 ± 0.20	—22 16 55.0 ± 2.0				Cwd	9	OU—269
1858—216	2		1.2	50	29	40 ± 15	114	29	35 ± 13			S		18 58 25.17 ± 0.20	—21 38 20.4 ± 4.0				Cwd	12	
1958—179	4		0.7	36	7.8	≤ 9.0	66	15	≤ 9.0			U		19 58 04.89 ± 0.15	—17 57 17.0 ± 3.0	+4.3	—0.6	18	†QSO(10)	23	OV-198
2041—149	3	S	1.6	18	2.0	1.6 ± 0.9				28	108	D	CN	20 41 29.83 ± 0.10	—14 56 36.3 ± 1.0					32	OW—169,
		A	0.8	28	2.1	≤ 2.5	92	2.0	≤ 1.5				A	20 41 29.07 ± 0.07	—14 56 33.0 ± 0.5	(—1	0)	20.5	†RO		MSH20—109
		B	0.8	28	2.1	≤ 2.5	92	7.8	18.5 ± 5.5				B	20 41 30.91 ± 0.15	—14 56 41.7 ± 1.0						
*2059—135	2		3.5							300	105	D	CN	20 59 00.00 ± 1.00	—13 30 20 ± 30	+9.0	+18.2	15.5	†EG(1)	35	PKS,
		A	1.4	47	20	60 ± 10	59	30	70 ± 15				A	20 58 50.20 ± 0.60	—13 29 40 ± 15						MSH20—119
		B	1.4	47	40	≤ 40	59	30	75 ± 15				B	20 59 10.00 ± 1.00	—13 31 00 ± 30						
2225—055	5		1.1							49.5	7	D	CN	22 25 50.55 ± 0.20	—05 33 53.0 ± 3.0	(+5	—2)	19.5	†RG?	50	4C-05.93
		A	0.7	0	15	20 ± 10	114	8.0	15.0 ± 5.0				A	22 25 50.40 ± 0.30	—05 34 10.0 ± 4.0						
		B	0.4	0	15	30 ± 15	114	8.0	13.0 ± 5.0				B	22 25 50.80 ± 0.30	—05 33 21.0 ± 4.0						
2236—039	6		1.0	22	4.2	6.5 ± 2.5	93	3.3	≤ 3.2			S		22 36 28.39 ± 0.04	—03 54 38.2 ± 0.7				EF	51	
*2243—032	9		3.5	22	0.8	≤ 0.5	107	0.8	≤ 0.7			HT		22 43 36.46 ± 0.02	—03 16 23.9 ± 0.7	+2.4	+1.0	19	†BO, G? (3)	52	4C-03.81
2300—013	5		1.0							32.5	20	D	CN	23 00 16.32 ± 0.10	—01 20 46.4 ± 1.5				EF	53	OZ-000
		A	0.5	20	8.3	7.5 ± 5.5	40	7.9	≤ 6.0				A	23 00 15.95 ± 0.08	—01 21 01.6 ± 1.1						
		A		68	7.9	≤ 9.0															
		B	0.5	20	6.4	≤ 6.5	40	7.9	8.0 ± 2.0				B	23 00 16.69 ± 0.08	—01 20 31.1 ± 1.1						
		B		68	7.9	≤ 5.5															
*2303—008	7		1.2							8.9	145	D	CN	23 03 11.77 ± 0.04	—00 52 21.4 ± 0.4	+1.7	+0.4	19	†G(9)	53	4C-01.59,
		A	0.6	11	4.1	≤ 3.5	104	3.1	≤ 3.0				A	23 03 11.65 ± 0.07	—00 52 18.0 ± 1.0						MSH 23-003
		A		160	4.0	7.6 ± 2.3															
		B	0.6	11	4.1	≤ 3.5	117	4.1	6.3 ± 2.5				B	23 03 11.99 ± 0.07	—00 52 25.3 ± 1.0						
		B		160	4.0	≤ 2.4															

(1)	(2)	(3)	(4)	(5)	(6)	(7)	(8)	(9)	(10)	(11)	(12)	(13)	(14)	(15)	(16)	(17)	(18)	(19)	(20)	(21)	(22)
2335+031	8		4.3	18 80	2.0 1.4	2.0 ± 0.3 1.6 ± 0.3	38 109	1.4 2.1	1.4 ± 0.3 1.5 ± 0.3		S			23 35 34.28 ± 0.03	+03 10 11.6 ± 0.4	+0.2	0.0	18	†BL Lac (12)	55	4C+03.59
*2338+030	2		3.0	11	1.3	0.8 ± 0.4	86	1.3	1.0 ± 0.6		Jets	20%		23 38 56.88 ± 0.07	+03 00 49.2 ± 1.0	+0.5	+1.7	19	†E3G(7)	55	4C+03.60

* Additional notes in text.

[a] Errors in Radio Position :— 0157+168 : ± 2 arcsec in PA 60 degree and ± 10 arcsec in PA 150 degree.

† A positive or likely identification

Finding Charts References :

1. Bolton and Ekers 1966
2. Clarke et al. 1966
3. Bolton and Ekers 1967
4. Merkelijn et al. 1968
5. Wills and Bolton 1969
6. Lang et al. 1970
7. Merkelijn and Wall 1970
8. Swarup et al. 1971
9. Wall 1971
10. Peterson et al. 1973
11. Slingo 1974
12. McEwan et al. 1975

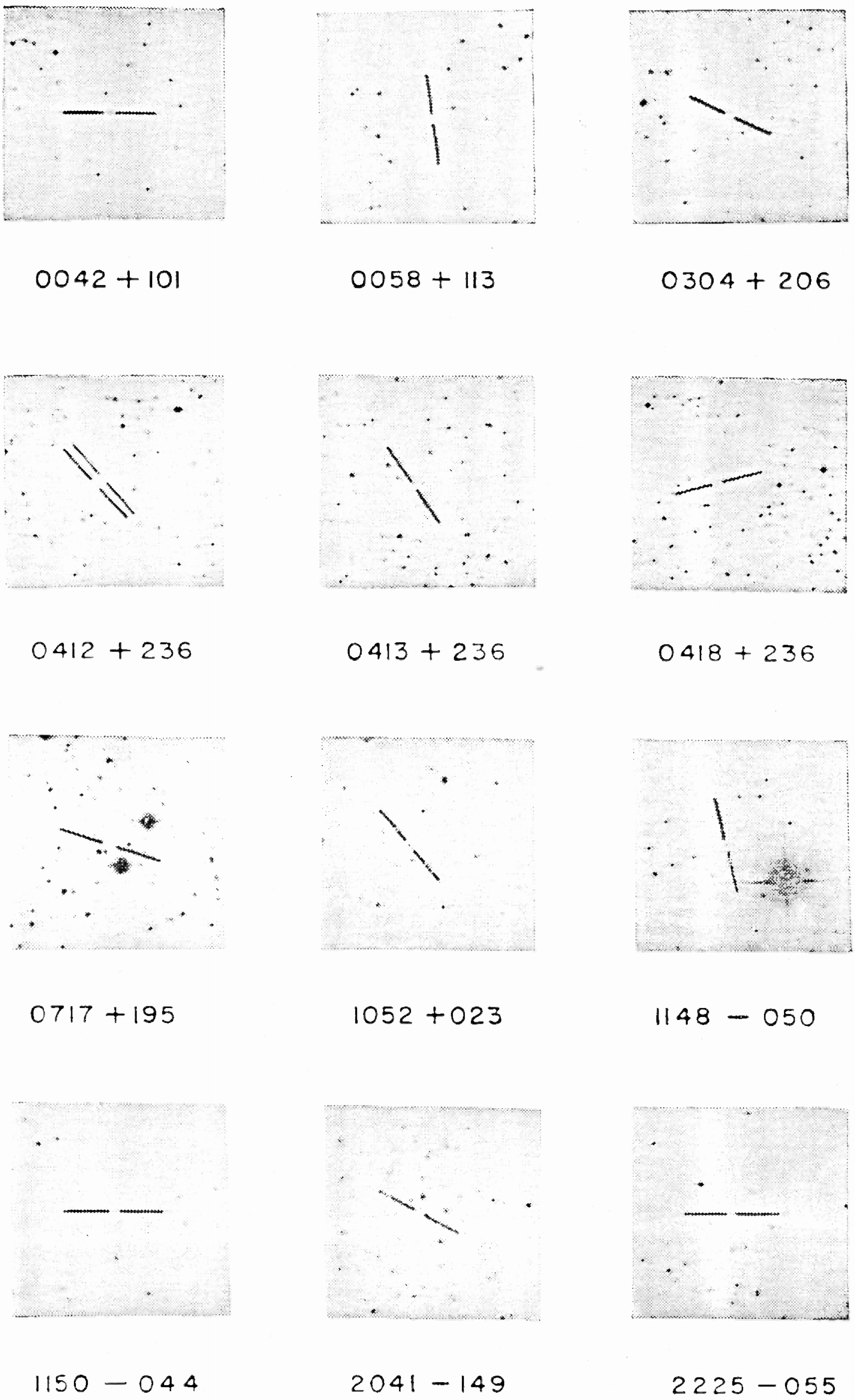

Plate 3.1: Finding charts for 12 radio sources. North is at top and east is at the left. The field shown covers about 10 arcmin on the side.

Table 3.2 Occultation data on 240 radio sources.

(1) Ooty name (OTL)	(2) No. of occ.	(3) Comp	(4) Flux den. Jy	(5) PA deg	(6) β_e ″	(7) Angular size ″ ″	(8) PA deg	(9) β_e ″	(10) Angular size ″ ″	(11) Overall Source Structure: LAS ″	(12) Overall Source Structure: PA deg	(13) Overall Source Structure: Notes	(14) Comp	(15) Radio position (1950.0) RA h m s s	(16) Radio position (1950.0) Dec ° ′ ″ ″	(17) Rad-Opt ΔRA ″	(18) Rad-Opt ΔDec ″	(19) Optical object m_{pg}	(20) Optical object Notes	(21) b^{II} deg	(22) Other Catalogue names
0002+041	3		0.6	39	5.8	≤4.7	87	15	12.9±3.2			PD, 1:1.5		00 02 40.80±0.05	+04 08 29.6±1.4				EF	57	
0007+051	3		0.65							29	173	D	CN	00 07 00.70±0.10	+05 09 02.5±2.0				EF	56	
		A	0.3	93	4.1	≤5.6	179	10	≤15				A	00 07 00.58±0.12	+05 09 17.5±2.0						
		B	0.35	93	4.1	≤7.5	179	10	≤11				B	00 07 00.81±0.12	+05 08 48.5±2.0						
0008+052	4		0.45	26	2.9	≤2.1	83	5.8	≤4.4			U		00 08 41.98±0.05	+05 16 31.7±0.8				EF	56	
0010+053	2		0.35	31	29	≤24	97	29	≤18			U		00 10 54.92±0.16	+05 21 43.7±5.2				EF	56	
0014+057	2		0.45							89	158	D	CN	00 14 11.27±0.30	+05 43 06.5±5.5					56	
		A	0.3	38	15	≤11	101	15	≤11				A	00 14 10.50±0.12	+05 43 35.5±2.5	(+2	+12)	20	†BG,CI		
		B	0.15	30	29	≤48	108	29	≤47				B	00 14 12.70±0.50	+05 42 13.0±9.5						
*0016+054	2		0.65	13	3.9	≤3.0	97	3.9	≤3.1			U		00 16 55.32±0.06	+05 26 43.5±0.8				EF	56	
0019+058	3		0.3	17	7.1	≤4.5	79	5.8	≤3.5			U		00 19 58.11±0.05	+05 51 27.0±1.0	(0	+1)	19.5	†BSO(1)	56	OB 034
0022+064	2		0.35	41	15	≤13	69	7.9	≤6.3			U		00 22 03.28±0.16	+06 26 48.7±4.6				EF	56	
0044+086	2		0.25	25	19	≤19	118	19	≤20			U		00 44 56.97±0.17	+08 40 06.7±2.6				EF	54	
0045+076	2		0.9	42	15	15.7 ±4.3	89	7.8	10.0±2.9			S		00 45 57.19±0.07	+07 41 33.1±1.8	(—1	+4)	20	†RG	55	4C+07.01
0052+075	3		0.4	33	15	14.5 ±8.3	80	7.8	≤6.0			S		00 52 07.19±0.08	+07 34 40.6±2.3				EF	55	
0053+090	2		0.3	49	7.8	≤7.7	62	15	<11			U		00 53 47.25±0.44	+09 03 21.0±8.5				EF	54	
*0054+078.1	2		0.65	127	3.9	≤5.0	167	3.9	≤4.3			U		00 54 42.71±0.10	+07 49 25.0±1.0				EF	55	
*0054+078.2	2		0.75	11	7.8	≤6.0	104	5.9	≤3.7			U		00 54 45.42±0.08	+07 53 48.3±1.0				EF	55	OB 091
*0054+090	4		2.4							16	35	D	CN	00 54 53.35±0.07	+09 01 41.8±1.0				EF	54	4C+09.03
		A	1.6	15	4.0	4.0 ±1.0	105	4.0	3.0±1.0				A	00 54 53.24±0.07	+09 01 39.0±1.0						
0058+097	2		0.5	56	5.9	≤6.7	81	5.8	≤4.3			U		00 58 28.27±0.09	+09 47 58.8±3.1				EF	53	
0109+105	2		0.5	52	29	≤20	60	7.9	8.4±5.5			S		01 09 34.17±0.78	+10 35 59.5±19	(—2	—2)	20.5	†G,CI	52	MC2
0112+104	2		0.4	7	15	17.4 ±6.7	116	15	14.6±7.8			PD		01 12 58.31±0.15	+10 28 33.0±2.0	(+6	+2)	21	†BO	52	MC2
*0116+111	2		0.7	52	29	36.5 ±8.2	96	39	43.1±7.7			Cx		01 16 22.61±0.14	+11 07 37.2±4.5	—4.5	—2.4	19.5	†RG,CI	51	
0118+104	3		0.25	54	15	≤14	77	29	≤22			U		01 18 29.78±0.25	+10 28 17.5±7.0				EF	52	MC2
0119+104	4		0.55	46	2.0	≤1.6	103	3.9	≤4.3			U		01 19 35.01±0.03	+10 25 21.4±0.9				EF	52	MC2
0146+133	2		0.75	67	9.8	11.5 ±4.2	85	20	29.5±5.0			S		01 46 46.05±0.14	+13 19 46.8±5.9	+5.5	—14.0	19.5	†BG	47	

(1)	(2)	(3)	(4)	(5)	(6)	(7)	(8)	(9)	(10)	(11)	(12)	(13)	(14)	(15)	(16)	(17)	(18)	(19)	(20)	(21)	(22)
*0153+136	2	S	2.0	31	15	15.0±5.0	115	29	25 ±10	25	150	D	CN	01 53 26.64±0.15	+13 41 33.9±1.5				EF	46	4C+13.11
*0156+126	3	S	1.0	111	2.9	3.3±0.8				42	21	D	CN	01 56 28.13±0.07	+12 38 01.4±1.1				EF	47	4C+12.09
		A	0.5	38	5.8	7.5±3.3							A	01 56 27.66±0.10	+12 37 43.3±1.0						
		B	0.5	38	7.8	10.8±3.3							B	01 56 28.70±0.10	+12 38 22.7±1.0						
*0156+136	2		1.2	55	5.9	≤5.6	68	2.0	≤1.3			U		01 56 57.35±0.14	+13 37 35.9±4.0				EF	46	
0158+137	2		0.55	50	15	≤15	71	7.8	7.5±6.2			S		01 58 12.19±0.17	+13 46 29.0±5.0	(0	—5)	20.5	†BG, C1?	46	
*0200+130	2	S	1.6	15	7.8	13.0±5.0	108	39	45 ±10			D,1:1.25	CN	02 00 54.00±0.20	+13 01 16.0±4.0				EF	46	4C+12.10
*0202+149	2		4.3	24	0.8	≤0.8	118	0.8	≤0.8			U		02 02 07.47±0.05	+14 59 50.3±0.7				EF	44	4C+15.05, NRAO91
0206+136	2		1.0	9	7.8	12.5±3.0	148	7.8	25.0±5.0			S		02 06 53.72±0.30	+13 37 47.0±1.5	(+2	—3)	20	†G	45	OD 111
0214+146	2		0.35	5	9.8	≤7.6	118	9.8	≤7.7			U		02 14 01.93±0.09	+14 41 01.8±1.4				EF	43	
0215+151	2		1.0	49	5.9	≤6.2	77	5.9	≤5.9			U		02 15 15.52±0.08	+15 08 43.2±2.1				EF	43	OD 125
*0232+150	2		1.15	53	7.8	8.5±2.0	82	5.9	5.4±2.0			S		02 32 37.56±0.06	+15 03 27.8±1.8				EF	41	
0235+153	2		0.5	74	7.8	≤8.0	82	5.9	7.3±3.6			S		02 35 33.25±0.15	+15 21 48 ±10				EF	40	OD+158.9
0237+154	2		2.4							6	82	D	CN	02 37 28.69±0.10	+15 26 15 ±10				EF	40	4C+15.08
		A	1.6	80	1.1	1.2±0.6	84	2.0	3.3±0.9				A	02 37 28.57±0.12	+15 26 15 ±10						
		B	0.8	80	2.0	≤1.5	84	2.0	≤1.6				B	02 37 28.93±0.10	+15 26 15 ±10						
0239+164	3		0.3	25	15	≤14	107	30	≤19			U		02 39 26.30±0.14	+16 24 48.9±2.1				EF	39	MC3
0249+171	2		0.5	24	5.9	≤7.0	108	7.9	≤9.6			U		02 49 19.85±0.08	+17 06 26.3±1.0	—1.0	+0.9	19.5	†G	37	MC3
*0255+173	2		0.55	81	29	26±16	87	29	≤29			PD		02 55 27.30±0.31	+17 19 33 ±37				INP	36	MC3
0305+173	2		0.25	21	29	≤30	112	29	≤35			U		03 05 52.80±0.40	+17 18 54.5±6.0				EF	34	
0309+175	2		0.9	62	2.2	≤2.5	81	3.0	≤2.7			U		03 09 57.73±0.06	+17 34 12.7±2.3	+3.7	+0.2	19	†G	34	MC3
0311+175.1	2		0.8	59	3.9	≤4.1	91	20	30.0±4.0			S		03 11 07.94±0.08	+17 32 02.8±2.4				EF	33	MC3
0311+175.2	2		0.8							9.4	101	D	CN	03 11 51.94±0.05	+17 32 57.3±1.4				EF	33	MC3
		A	0.55	56	3.0	≤2.0	100	3.9	5.3±2.3				A	03 11 51.83±0.04	+17 32 57.8±1.2						
		B	0.25	56	3.0	≤2.5	100	3.9	≤4.2				B	03 11 52.47±0.06	+17 32 56.0±1.7						
*0312+180	2		1.4	59	3.9	≤3.5	113	3.9	≤3.3			U		03 12 05.16±0.04	+18 02 43.3±1.1				EF	33	H, OE+120
0319+173	2		0.25	45	9.8	≤7.6	90	9.8	≤13			U		03 19 03.48±0.09	+17 19 50.3±2.4				EF	32	
0320+184	2		0.2	33	30	≤22	103	30	≤24			U		03 20 53.31±0.25	+18 26 43.1±4.1				EF	31	
*0325+180	2		1.2	11	10	≤10	142	10	≤10			U		03 25 22.15±0.50	+18 00 44.0±4.0				EF	31	4C+18.09
*0325+179	2		0.7	32	15	≤15	122	15	≤15			U		03 25 32.63±0.10	+17 58 01.8±1.5	(—2	+4)	20	†BG	31	4C+18.09
0325+176	2		0.4	72	29	≤20	93	9.8	≤7.5			U		03 25 41.37±0.08	+17 40 24.5±8.0	(+3	+15)	21	BO	31	

(1)	(2)	(3)	(4)	(5)	(6)	(7)	(8)	(9)	(10)	(11)	(12)	(13)	(14)	(15)	(16)	(17)	(18)	(19)	(20)	(21)	(22)
*0329+175	2		0.7	36	5.9	≤6.2	141	5.9	≤5.4			U		03 29 03.80±0.08	+17 34 49.3±0.9				EF	31	MC3
0335+188	2		0.35	77	30	≤26	89	15	≤15			U		03 35 00.44±0.18	+18 51 38 ±26				EF	29	
0342+199	2		0.8	7	3.0	4.7±1.5	134	3.0	≤3.0			PD, 3:1		03 42 20.04±0.10	+19 56 39.1±1.0				EF	27	OE 170.2
*0343+184	2		0.8							122	176	D	CN	03 43 23.78±1.00	+18 26 06.3±2.2				EF	28	H
		A	0.35	48	9.8	≤9.7	113	5.9	≤4.7				A	03 43 23.51±0.07	+18 27 03.3±1.8						
		B	0.45	37	3.0	≤3.0	124	5.9	≤4.5				B	03 43 24.08±0.07	+18 25 01.9±1.2						
0345+195	2		0.45	25	9.8	≤9.2	142	15	21.0±6.0			S		03 45 10.78±0.15	+19 32 58.5±1.2				EF	27	OE 176
0345+186	2		0.3	83	15	≤13	91	15	≤12			U		03 45 20.10±0.25	+18 39 45 ±30	+0.5	+5.1	19	†RG	27	
*0359+193	2		1.4									HT ?, Cx	CN	03 59 18.85±0.20	+19 21 12.0±6.0	+4.5	−6.2	14.5	NSO	24	4C+19.10
		A	0.5	38	8.0	≤7.0	105	8.0	≤7.0				A	03 59 17.20±0.15	+19 21 13.0±2.0						
0429+201	2	S	1.35	123	4.0	4.2±2.1				8.8	33	D	CN	04 29 58.52±0.07	+20 06 53.2±1.2				EF	19	OF 150.1, H
		A	0.8	58	4.0	≤2.3							A	04 29 58.43±0.07	+20 06 51.3±1.0						
		B	0.55	58	4.0	≤3.5							B	04 29 58.76±0.08	+20 06 58.6±1.2						
0431+196	2		0.4	73	5.9	≤4.0	78	5.9	≤8.0			U		04 31 23.70±0.30	+19 40 27 ±16				EF	19	
*0436+203	3		1.6	50	20	43.0±4.0	113	30	32.0±5.0			S		04 36 49.06±0.08	+20 18 08.4±1.6				EF	17	4C+20.14
0437+205	2		0.65	54	2.0	≤2.1	111	5.9	7.3±2.7			S		04 37 15.45±0.05	+20 35 03.7±1.0	−0.7	+2.0	20.5	†RO	17	OF 263
0440+197	2		0.4	84	30	≤32	108	30	≤28			U		04 40 41.10±0.25	+19 44 53 ±19				EF	17	
0452+207	2		0.65	80	40	50 ±10						PD, 1:1		04 52 51.60±0.50	+20 43 00 ±30				EF	14	OF 288
0453+205	4		1.8	40	6.0	16.0±3.0	73	4.0	≤5.5			S		04 53 31.89±0.03	+20 34 15.7±0.8				EF	14	4C+20.16
				101	4.0	6.2±2.0	123	6.0	8.7±1.5												
*0455+201	2		0.7	35	3.0	≤3.2	126	4.0	≤4.5			U		04 55 32.59±0.07	+20 07 04.9±1.0				EF	14	
0506+198	4		0.6	72	4.0	≤4.0	87	4.0	≤4.0			U		05 06 03.67±0.07	+19 53 54.0±4.0				EF	12	OG 110
0512+209	2		0.85	55	20	27.5±4.5	110	4.0	≤3.2			S		05 12 48.96±0.06	+20 54 26.8±1.8				EF	10	
0513+198	2	S	0.8	70	15	≤16	125	30	28.0±7.0	28	125	D,2:1	CN	05 13 04.81±0.12	+19 49 21.4±2.9				EF	11	
0514+209	2		0.9	61	15	27.5±3.0	111	8.0	8.5±2.5			S		05 14 30.49±0.05	+20 57 45.6±1.6	+4.0	−6.7	19.5	RG	10	
0518+195	3		0.5	70	30	≤30	141	30	≤30			U		05 18 05.20±0.20	+19 34 54.9±3.0	+9.7	−9.8	16	NSO	10	
0518+198	3		0.6	83	7.9	8.3±3.4	126	7.9	6.1±4.3			S		05 18 20.61±0.07	+19 48 54.9±1.5				EF	10	OG 131?
*0519+196	3		1.3	87	2.0	≤2.0	117	3.0	≤3.0			U		05 19 07.85±0.04	+19 38 02.8±1.5				EF	10	4C+19.14
0525+199	2		0.75	39	2.0	≤1.9	126	2.0	≤1.3			U		05 25 36.41±0.05	+19 54 19.3±0.8				EF	8	
*0529+198	2		2.4							7.6	77	D	CN	05 29 21.54±0.05	+19 49 26.7±1.0				EF	7	H, OG 149
		A	1.2	56	3.0	1.9±1.3	123	2.0	≤2.2				A	05 29 21.26±0.05	+19 49 25.9±0.8						
		B	1.2	56	2.0	2.3±0.7	123	2.0	1.9±0.9				B	05 29 24.78±0.05	+19 49 27.6±0.8						

TABLE 3.2 (Contd.)

(1)	(2)	(3)	(4)	(5)	(6)	(7)	(8)	(9)	(10)	(11)	(12)	(13)	(14)	(15)	(16)	(17)	(18)	(19)	(20)	(21)	(22)
0534+198	2		1.05	74	30	29.0±7.0	130	30	25.0±8.0			PD, 1:1	CN	05 34 44.48±0.10	+19 51 37.0±2.4				EF	6	H
*0539+198	2	S	2.0	90	20	20.0±5.0						D, 1:1	CN	05 39 18.40±0.40	+19 49 15 ±60				INP	5	4C+19.16
0546+205	2		0.95	68	4.0	≤4.8	102	4.0	≤3.1			U		05 46 38.30±0.04	+20 30 36.2±1.7				EF	4	
0551+205	2		1.5	84	4.1	5.0±2.5	107	8.0	15.8±3.0			S		05 51 32.96±0.05	+20 30 23.1±2.4	+1.1	—3.7	19.5	RO,Cwd	3	OG 286
0618+197	2	S	1.7	103	6.0	6.8±1.5	112	6.0	8.5±2.5			D,1:1	CN	06 18 13.05±0.12	+19 45 15.8±5.6				Cwd	3	4C+19.20
0620+197	2		0.5	52	10	≤11	161	4.0	<3.2			U		06 20 48.72±0.11	+19 46 14.8±0.8				EF	3	
*0628+191	3		2.5	65	40	75±15	113	20	25.0±5.0			HT?,Cx		06 28 35.79±0.15	+19 10 56.7±2.5	+2.1	+4.7	16	†RG	4	4C+19.21
				148	30	40±15															
0629+189	2		0.55	102	7.9	<5.5	113	9.9	<5.2			U		06 29 57.62±0.14	+18 55 53.8±5.9				EF	5	
0631+192	4		2.2	54	4.0	≤2.9	140	15	15.0±5.0			PD, 1:1		06 31 54.61±0.07	+19 12 04.3±1.2				EF	5	
0632+189	4		3.0	89	2.1	1.2±0.6	164	2.0	1.5±0.7			PD, 1:4		06 32 25.44±0.03	+18 57 42.2±0.5				EF	5	4C+19.22
0635+191	3	S	1.5	133	4.0	5.0±1.0				30	49	D	CN	06 35 48.55±0.07	+19 08 22.8±1.2	—3.8	—0.4	19.5	†BSO	6	4C+19.23
		A	1.0	84	6.0	6.7±2.3							A	06 35 48.15±0.06	+19 08 18.5±1.2						
		B	0.5	84	6.0	≤7.6							B	06 35 49.76±0.07	+19 08 38.0±1.5						
0644+192	2		1.45	89	6.0	5.5±2.5	116	6.0	8.5±2.5			PD		06 44 03.84±0.05	+19 17 53.2±2.2				EF	8	4C+19.24
0645+189	2	S	1.2	28	2.0	≤1.4				11.3	117	D	CN	06 45 04.49±0.08	+18 56 34.6±0.6					8	H
		A	0.5	157	6.0	≤5.3							A	06 45 04.10±0.10	+18 56 37.4±0.7	+1.6	+1.3	19.5	†RG?,Cwd		
		B	0.7	157	6.0	≤4.4							B	06 45 04.81±0.08	+18 56 32.3±0.6						
0646+184	4		1.4	55	3.0	3.0±1.8	160	2.0	2.2±0.8			S		06 46 40.48±0.03	+18 25 36.8±0.4				EF	8	4C+18.19
0647+192	2		0.4	76	10	<12						U		06 47 37.64±0.16	+19 13 52.0±8.5				EF	8	
0652+187	2		0.75	81	30	53±10	122	30	24±12			S		06 52 21.72±0.15	+18 44 56.2±4.6	+5.7	—1.4	16	†RG,Cwd	9	
0702+181	2		0.6	90	8.1	≤6.1	135	15	<12			U		07 02 53.25±0.10	+18 08 02.9±3.4	(+2	—2)	20.5	†BO	11	OI 105
*0708+184	3		2.2							16	135	D	CN	07 08 06.15±0.05	+18 24 38.4±1.0	(—2	0)	20.5	†RO	12	4C+18.20
		A	1.3	32	2.3	3.2±0.8	80	2.0	1.9±1.5				A	07 08 05.90±0.07	+18 24 42.0±1.0						
0727+174	2		0.4	102	10	≤8.1	117	8.1	<8.0			U		07 27 51.68±0.21	+17 27 17.5±7.5	—0.3	+6.3	15.5	†NSO	16	
0731+169	2		0.35	92	10	≤7.5	136	15	≤16			U		07 31 45.72±0.11	+16 55 21.2±3.3	(—1	—5)	21	†BO	17	
0736+167	5		1.8							4	23	D	CN	07 36 33.08±0.03	+16 42 04.4±0.6				EF	18	4C+16.22
		A	0.4	81	1.3	≤1.0	173	2.0	≤1.7				A	07 36 33.00±0.10	+16 42 01.0±1.5						
		B	1.4	81	1.3	≤1.0	173	2.0	≤1.7				B	07 36 33.11±0.04	+16 42 04.8±0.7						
0746+162	5		1.4	19	2.1	3.4±0.8	87	3.0	2.3±1.2			PD, 1:5		07 46 06.93±0.02	+16 17 28.1±0.5				EF	20	4C+16.23
0748+164	6		1.9	101	2.1	≤2.0	122	2.1	<2.0			U		07 48 12.77±0.04	+16 28 16.2±1.5	(0	+2)	21	†BO	20	4C+16.24
*0806+152	8		1.5							26.5	139	D	CN	08 06 04.78±0.04	+15 16 34.6±0.8	(+7	0)	20.5	RO	24	4C+15.22
		A	0.9	95	4.0	5.5±2.0	151	4.0	4.8±2.4				A	08 06 04.26±0.03	+15 16 41.6±0.6						
		B	0.6	95	3.0	≤3.5	151	4.0	≤2.9				B	08 06 05.46±0.03	+15 16 21.8±0.6						

(1)	(2)	(3)	(4)	(5)	(6)	(7)	(8)	(9)	(10)	(11)	(12)	(13)	(14)	(15)	(16)	(17)	(18)	(19)	(20)	(21)	(22)
0822+144	2		0.45	80	10	<10	142	15	<14			U		08 22 57.81±0.08	+14 28 27.3±2.3	(−3	+2)	21	†BG	27	
0823+140	2		0.3	62	10	≤7.8	164	6.1	≤5.4			U		08 23 02.82±0.10	+14 05 40.3±0.9				EF	27	
0852+124	5	S	0.9	91	2.1	2.7±1.0				12.7	9	D	CN	08 52 37.03±0.04	+12 28 56.0±1.0				EF	33	4C+12.32
		A	0.5	145	2.1	<2.1							A	08 52 36.95±0.10	+12 28 50.5±1.5						
		B	0.4	145	4.1	≤4.3							B	08 52 37.09±0.10	+12 29 03.0±1.5						
0853+124	5		0.7	80	30	120±20	150	15	22.0±5.0			S		08 53 09.80±0.50	+12 24 59.0±5.0	(+8	−8)	17.5	RO	33	OJ 189.2
0853+121	6		0.75	76	4.0	≤4.7	150	8.0	≤9.0			U		08 53 12.91±0.05	+12 08 21.1±0.7				EF	33	
0855+122	6		0.5	70	6.0	≤5.0	158	4.0	≤3.1			U		08 55 00.96±0.03	+12 12 57.2±0.5				EF	33	
0912+105	2		0.85	120	8.0	≤6.4	154	8.0	10.5±2.5			S		09 12 31.08±0.12	+10 30 57.7±1.5				EF	37	
0914+103	2		0.8	120	15	15.0±5.0						S		09 14 03.35±0.50	+10 18 51 ±16				INP	37	
0915+099	2		0.9	100	6.0	≤6.5	131	30	≤31			U		09 15 57.27±0.10	+09 59 37.2±5.6				EF	37	OK 026
0920+104	4		0.35	77	8.0	<5.9	156	4.0	≤2.5			U		09 20 37.64±0.05	+10 24 59.4±0.7	(+1	−2)	20.5	†BO	38	
*0925+092	5	S	1.5	83	3.1	2.0±1.5	177	10	12.5±2.5			D	CN	09 25 14.79±0.02	+09 17 35.5±0.5				EF	39	4C+09.34
0926+092	7		0.7	115	20	25±10	175	15	20±10			PD, 1:1		09 26 50.59±0.07	+09 16 44.0±1.5	+4.6	−9.2	19	NSO	39	
0932+089	2		2.8	74	6.1	5.9±1.0	160	3.0	2.6±0.6			PD, 2:1		09 32 24.13±0.03	+08 55 02.6±0.5	(−1	−1)	20.5	†RO(2)	40	4C+08.31
*0946+076	2		2.1							70	150	D	CN	09 46 17.40±0.30	+07 41 48 ±10	(0	+1)	20.5	†RG,C1?	43	NRAO 336, OK 77
		A	1.1	110	4.1	7.5±2.0	130	3.1	4.5±1.5				A	09 46 16.70±0.10	+07 42 08.3±2.3						
		B	0.6	109	15	<15	131	30	≤30				B	09 46 19.00±0.55	+07 41 08 ±22						
*0949+077	2	S	0.7	120	30	45 ±15						D, 1:1	CN	09 49 58.50±1.00	+07 43 40 ±30	+23.8	+2.6	20	RG	43	OK 083
0955+070	3		0.45	90	4.4	≤4.0	132	10	≤7.8			U		09 55 51.08±0.06	+07 05 52.1±2.4				EF	44	
1007+062	2		1.45							30	52	D	CN	10 07 18.77±0.08	+06 16 07.1±1.0				EF	46	OL 012
		A	1.05	1	2.1	1.6±1.4	60	3.0	3.8±1.0				A	10 07 18.32±0.05	+06 16 01.9±0.5						
		B	0.4	4	6.1	6.5±3.3	57	10	≤10				B	10 07 19.89±0.13	+06 16 20.2±1.0						
1013+054	2		0.3	92	21	≤14	141	15	≤9.5			U		10 13 26.89±0.16	+05 28 06.0±2.6	(+4	+6)	20	†BO	47	
*1033+038	4		0.85	5	6.1	6.2±2.9	54	10	15.5±3.5			PD		10 33 02.16±0.06	+03 53 57.0±1.0				EF	50	
				112	6.1	8.2±3.4															
*1039+035	3		1.1									HT?, Cx	CN	10 39 33.34±0.07	+03 30 32.8±1.2				EF	51	OL 066.3
		A	0.4	93	6.1	<5.7	168	6.1	≤4.2				A	10 39 32.32±0.06	+03 30 27.0±1.2						
*1048+022	4		0.5	78	20	≤21	149	20	≤21			U		10 48 41.54±0.08	+02 14 26.5±2.3				EF	52	
1121−007	2		0.35	117	21	≤19						U		11 21 38.75±0.67	−00 43 53 ±40				EF	55	
1123−010	2		0.2	93	31	<30	135	31	≤30			U		11 23 37.40±0.50	−01 04 45.5±8.0	(−16	+14)	21	BO	55	
1123−008	2		0.25	90	31	<36	138	31	<35			U		11 23 52.85±0.35	−00 52 21.5±7.5				EF	55	

(1)	(2)	(3)	(4)	(5)	(6)	(7)	(8)	(9)	(10)	(11)	(12)	(13)	(14)	(15)	(16)	(17)	(18)	(19)	(20)	(21)	(22)
1150—036	2		0.95							34	39	D	CN	11 50 18.01±0.13	03 38 48.1±2.6				EF	56	OM—083
		A	0.35	78	15	≤15	168	15	≤18				A	11 50 16.82±0.21	—03 38 58.6±2.5						
		B	0.6	78	15	≤11	168	6.2	≤5.0				B	11 50 18.27±0.09	—03 38 32.2±0.9						
*1201—041	2		4.5							21	71	Cx	CN	12 01 28.46±0.12	—01 06 01.5±2.5	+4.5	+1.0	18	†RG,CI(3)	56	4C—04.40
		A	1.5	46	3.1	8.5±2.5	111	3.3	6.3±1.7				A	12 01 27.69±0.10	—04 06 07.8±2.2						
		B	1.5	46	2.1	6.0±1.7	111	3.3	5.3±1.7				B	12 01 28.50±0.12	—04 06 01.4±2.5						
		C	1.5	46	2.1	6.3±1.7	111	3.3	7.0±2.0				C	12 01 29.03±0.13	—04 06 00.8±2.8						
*1220—059	2		1.6							150	107	D, Br15%	CN	12 20 10.10±1.00	—05 59 25 ±30	—55.3	+6.7	19	†G	56	4C—05.50
		A	0.9	112	15	30.0±7.0	121	15	30.0±7.0				A	12 20 06.30±0.90	—05 59 05 ±25						
		B	0.5	114	6.2	≤4.9	119	6.0	≤5.2				B	12 20 16.00±0.50	—05 59 50 ±15						
1232—064	2		0.75	78	3.1	≤2.5	164	4.1	≤2.8			U		12 32 26.37±0.05	—06 27 41.2±0.8				EF	56	ON—054
1238—074	2		0.6	81	6.1	≤4.0	135	6.1	≤5.3			U		12 38 12.52±0.05	—07 26 47.6±1.4				EF	55	
1244—079	2		1.1	118	16	13.0±8.0	126	16	≤11			S		12 44 21.97±0.54	—07 56 44 ±13	+0.5	—10.0	18.5	†G	55	ON—074
1245—075	2		0.35	102	15	≤12	136	21	40±10			S		12 45 12.28±0.19	—07 33 02.3±6.0	(—6 (+6	+5) +6)	20 20.5	†RG †RG	55	
1246—081	2	S	1.0	101	30	35±10	141	8.2	11.7±4.7			D, 1:1	CN	12 46 15.40±0.20	—08 06 12.0±3.0				EF	55	ON—077
1249—086	2		1.1	114	31	90±15						S		12 49 43.5 ±2.0	—08 39 30 ±60				INP	54	ON—084
1253—089	2		0.3	83	20	≤27	139	20	≤19			U		12 53 43.33±0.16	—08 55 09.6±3.1				EF	54	
1256—092	2	S	0.8	48	15	20±10	166	30	45±20			D, 1:1	CN	12 56 16.40±0.25	—09 14 45.5±3.0	+1.0	+5.0	20	†RG	53	ON—093
1313—107	2		0.6	73	10	≤10	139	4.1	≤3.2			U		13 13 56.68±0.08	—10 43 49.7±1.2				EF	51	
1321—114	2		0.45	105	31	≤40	136	31	≤22			U		13 21 03.80±0.30	—11 27 25.0±7.0	(+14	—4)	21	BO	50	
1322—116	2	S	2.0	102	3.1	3.4±1.5	139	6.1	7.6±2.0			D	CN	13 22 08.21±0.05	—11 37 54.1±1.3				EF	50	OP—137
1325—115	2		0.6	58	10	15.0±5.0	150	31	24±12			S		13 25 08.75±0.25	—11 32 01.0±5.0	—0.4	+5.0	19.5	†BG	50	
*1339—121.1	2		2.0	102	2.1	≤2.0	132	2.1	≤1.3			U		13 39 26.31±0.05	—12 10 31.5±1.3				EF	49	PKS
*1339—121.2	2		0.5	108	15	≤8.2	127	4.1	≤3.2			U		13 39 50.28±0.15	—12 11 41.3±3.8				EF	49	
1343—124	4		1.0	118	8.3	10.0±3.5	173	8.2	9.5±2.5			PD, 1:1		13 43 50.08±0.04	—12 24 46.2±0.6				EF	48	OP—173
1344—127	2		1.1	107	3.2	≤2.2	128	6.2	≤2.7			U		13 44 15.23±0.08	—12 46 51.1±2.2				EF	48	OP—173
*1348—129	6		3.5	75	1.1	1.2±0.3	152	1.0	≤0.4			S		13 48 09.30±0.03	—12 57 19.1±0.5				EF	47	PKS
1354—132	2		0.35	85	31	≤30	121	4.1	≤3.2			U		13 54 36.38±0.11	—13 12 37.1±3.0				EF	46	
*1416—156	2	S	3.2	101	15	20.0±3.0	119	20	25.0±3.0			Cx	CN	14 16 15.55±0.10	—15 41 42.5±5.0	(—2	—2)	20.5	†RG	42	MSH 14—104, PKS
1421—152	2		0.45	88	8.2	≤9.0	125	8.3	≤13			U		14 21 33.39±0.08	—15 12 06.5±2.8	(+1	—8)	21	†BO	42	
1422—153	2		0.4	72	15	≤11	137	16	<20			U		14 22 24.71±0.11	—15 19 20.1±2.6	(+4	+1)	21	†BO	42	

(1)	(2)	(3)	(4)	(5)	(6)	(7)	(8)	(9)	(10)	(11)	(12)	(13)	(14)	(15)	(16)	(17)	(18)	(19)	(20)	(21)	(22)
1422—150	2		1.6							150	8	D.	CN	14 22 51.05±0.15	—15 02 05.0±5.0				EF	42	OQ—138
		A	0.8	75	8.3	13.0±4.0	134	10	12.2±5.7			Br 25%	A	14 22 50.44±0.07	—15 03 07.1±1.9						
		B	0.4	65	21	29.0±7.0	141	15	≤15				B	14 22 51.92±0.12	—15 00 38.1±2.0						
1426—161	2		1.6	92	15	18.0±3.0	109	15	21.5±3.0			S		14 26 52.73±0.07	—16 09 33.8±4.4	+0.8	—8.5	18.5	†RG?	40	OQ—145
1429—154	2		0.85							27	172	D	CN	14 29 09.20±0.30	—15 26 19.0±6.0				EF	41	
		A	0.3	72	61	65±35	140	31	<30				A	14 29 09.05±0.45	—15 26 01.0±7.0						
		B	0.55	71	20	22±10	141	15	22.5±7.5				B	14 29 09.30±0.15	—15 26 28.0±3.0						
1434—155	2	S	1.0	87	61	66±12	109	61	64±20			D, 1:1	CN	14 34 12.00±0.20	—15 34 30 ±15	—1.6	+21.8	19.5	RG?	40	
1440—160	2		0.65	105	31	50±15	124	31	85±20			S		14 40 36.45±0.50	—16 05 55 ±20	(+4	—5)	20	†RG	39	
1445—166	2		0.65	108	10	≤13						U		14 45 22.15±0.50	—16 36 27 ±20				EF	38	
1445—161	4		2.8	108	1.2	≤1.0	115	0.8	≤0.5			U		14 45 28.44±0.11	—16 07 53.6±3.5	(+2	+3)	20.5	†RO	38	PKS
*1452—168	2		0.8	76	31	≤31	128	10	≤11			U		14 52 15.00±0.21	—16 48 01.8±4.1	(—1	—1)	20.5	†BO	27	OQ—189
*1456—165	2		1.5	21	2.1	≤2.0	172	4.1	3.0±1.5			S		14 56 21.26±0.14	—16 33 47.1±0.7	(+1	+2)	21	†BO	37	CUL1
1522—188	2		2.7	93	2.1	≤1.8	113	2.1	≤2.0			U		15 22 20.80±0.05	—18 52 19.1±2.5	(+1	—4)	20.5	†RO	31	PKS
1524—181	2		0.55	94	6.2	≤4.3	102	6.1	≤3.9			U		15 24 03.60±0.10	—18 10 58.5±9.0	(+3	—5)	20.5	†RO	31	
1531—182	2		0.55	82	41	≤37	108	15	≤11			U		15 31 16.10±0.30	—18 17 53 ±12	—6.7	—6.6	19	†NSO	30	
1548—199	2	S	1.1	121	8.2	≤10				20	31	D	CN	15 48 02.29±0.07	—19 55 15.9±2.6				EF	26	OR—280, MSH 15—116
		A	0.55	83	6.1	≤9.6							A	15 48 01.84±0.10	—19 55 26.4±4.0						
		B	0.55	83	6.1	≤5.9							B	15 48 02.58±0.10	—19 55 09.0±4.0						
1551—205	2		0.8	102	4.1	≤4.6	112	3.2	3.2±1.7			S		15 51 15.73±0.12	—20 32 05.5±4.9				EF	25	MC1
1551—207	2		0.35	137	6.0	≤5.7						U		15 51 56.30±0.50	—20 42 08.4±5.0				EF	25	MC1
1553—191	2		0.7	98	3.1	≤2.0						U		15 53 49.00±0.40	—19 07 00 ±30				EF	26	OR—190
1557—208	2		0.55	56	10	12.5±5.0	124	10	20.0±7.5			PD		15 57 41.46±0.15	—20 53 38.8±2.5	+14.0	—1.0	11	NSO	24	MC1
1601—209	2		0.75	24	4.0	≤3.0	150	6.0	≤5.6			U		16 01 01.31±0.09	—20 57 43.8±0.6				EF	23	MC1
1612—208	2		0.35	54	30	≤30	152	30	≤30			U		16 12 59.30±0.80	—20 50 48 ±12				INP	21	MC1
1614—208	2		0.25	76	60	≤60	125	40	≤40			U		16 14 02.70±0.70	—20 48 00 ±30	—5.3	—10.2	17	RG, INP	21	MC1
1615—201	2		1.05							53	173	D	CN	16 15 38.85±0.20	—20 10 30.7±3.0				EF	21	MC1
		A	0.65	50	15	≤15	113	10	12.0±7.0				A	16 15 38.43±0.12	—20 10 11.3±2.0						
		B	0.4	50	15	≤15	113	15	≤12				B	16 15 38.93±0.15	—20 11 04.0±3.8						
1617—206	2		0.2	74	60	≤60	105	90	≤90			U		16 17 49.15±1.00	—20 41 32 ±45				INP	20	MC1
1618—208	2		0.25	69	60	≤62	106	40	≤52			U		16 18 57.36±0.42	—20 50 39 ±18				INP	20	MC1
1621—196	3		0.55	94	21	22±12	112	15	≤17			S		16 21 40.20±0.40	—19 40 26.0±6.0				EF	20	MC1

(1)	(2)	(3)	(4)	(5)	(6)	(7)	(8)	(9)	(10)	(11)	(12)	(13)	(14)	(15)	(16)	(17)	(18)	(19)	(20)	(21)	(22)
1623—194	2		1.1							14	125	D	CN	16 23 29.35±0.08	—19 28 21.9±2.7				EF	20	MSH 16—110, OS—139.2
		A	0.8	89	6.1	≤8.3	121	8.2	8.5±4.0				A	16 23 29.17±0.07	—19 28 18.2±2.5						
		B	0.3	89	6.1	≤6.0	121	6.1	≤5.6				B	16 23 29.96±0.10	—19 28 26.1±3.4						
*1628—211	2		1.2	72	2.0	<1.7	138	2.0	≤2.0			U		16 28 52.97±0.06	—21 11 13.5±1.0				EF	18	MCI
1631—201	2		1.05							14.5	7	D	CN	16 31 42.25±0.10	—20 07 50.2±0.6	+2.4	—0.2	18	†RG	18	MCI
		A	0.6	33	8.2	≤11	149	6.2	≤6.5				A	16 31 42.17±0.10	—20 07 57.7±0.8						
		B	0.45	33	8.2	≤11	149	6.2	≤4.8				B	16 31 42.30±0.10	—20 07 43.2±0.8						
1632—199	4		1.0	56	6.1	≤3.4	110	4.1	3.5±2.0			S		16 32 49.05±0.03	—19 58 10.2±2.0				EF	18	MCI
1634—215	2	S	0.7	53	4.0	≤4.8				26	143	D	CN	16 34 34.47±0.09	—21 30 03.4±1.5				EF	17	MCI
		A	0.3	137	15	≤11							A	16 34 33.94±0.09	—21 29 53.6±1.6						
		B	0.4	140	15	27±12							B	16 34 35.05±0.13	—21 30 14.1±2.3						
1637—196	2		1.0	31	2.1	<1.7	139	10	≤10			U		16 37 43.12±0.25	—19 36 29.4±2.5				EF	17	OS—163, MSH 16—115
1651—200	2		0.55	94	15	≤15	109	21	28±10			S		16 51 29.60±0.25	—20 04 58 ±14				INP	15	
1653—201	2		0.25	84	31	≤35	116	30	≤30			U		16 53 02.95±0.30	—20 06 27 ±10				INP	14	MSH 16—211?
*1655—201	2		2.2									Cx	CN	16 55 07.31±0.10	—20 06 57.9±2.0					14	HM, OS—192
		A	1.1	66	3.1	4.2±1.4	128	4.1	4.3±1.7				A	16 55 07.37±0.06	—20 06 49.2±1.0	+1.0	—1.6	19.5	†G		
1657—203	2		0.8							43	28	D	CN	16 57 23.39±0.07	—20 20 37.1±5.5				INP	13	OS—296
		A	0.3	78	8.2	≤6.8	103	8.2	≤11				A	16 57 22.42±0.08	—20 21 00.8±5.3						
		B	0.5	81	6.2	≤5.3	101	6.2	≤5.3				B	16 57 23.87±0.05	—20 20 23.0±3.9						
1658—200	2		0.5	31	3.1	≤2.1	145	8.2	≤7.3			U		16 58 38.22±0.09	—20 03 39.6±0.7				EF	13	MOL
1700—204	2	S	1.8	128	1.1	1.3±0.5				5.1	38	D	CN	17 00 18.74±0.07	—20 27 26.7±1.0				EF	13	OT—200
		A	0.8	42	3.1	≤1.9							A	17 00 18.69±0.07	—20 27 27.6±1.0						
		B	1.0	42	3.1	≤2.5							B	17 00 18.92±0.07	—20 27 23.6±1.0						
1701—203	2		0.25	66	10	<7.7	101	15	≤12			U		17 01 33.53±0.11	—20 19 11.4±4.1	—5.3	+0.3	20	RO	13	MOL
1702—204	2		0.5	35	31	55±10	131	21	40±10			PD, 1:1		17 02 09.89±0.19	—20 25 33.3±2.5				INP	12	
1703—203	2		0.3	50	31	≤31	114	4.1	≤4.0			U		17 03 28.78±0.13	—20 19 39.9±4.0	—2.8	—6.6	19.5	RO	12	MOL
*1723—203	2		0.4	77	8.2	≤6.1	119	10	≤7.5			U		17 23 18.96±0.07	—20 19 53.1±2.7				INP	8	
1731—217	2		0.5	32	30	≤30	148	30	≤30			U		17 31 04.30±0.40	—21 44 48.0±3.0				Cwd	6	
1736—213	2		0.65	74	6.0	≤4.9	80	6.0	≤5.9			U		17 36 35.33±0.20	—21 21 01.5±12				Cwd	5	
1739—205	2		1.2	84	10	9.5±3.0	107	8.1	8.1±3.5			PD, 2:1		17 39 26.02±0.05	—20 35 59.3±3.1				Cwd	5	
1739—213	2		0.30	126	59	125±35						S		17 39 54.70±0.70	—21 21 56±10				Cwd	5	
1744—214	2		0.5	95	30	<30						U		17 44 48.80±0.20	—21 28 45±30				Cwd	3	

(1)	(2)	(3)	(4)	(5)	(6)	(7)	(8)	(9)	(10)	(11)	(12)	(13)	(14)	(15)	(16)	(17)	(18)	(19)	(20)	(21)	(22)
1750—216	2		0.35	39	15	≤12	124	15	≤12			U		17 50 13.47±0.14	—21 39 12.4±2.2				Cwd	2	
1807—207	2		2.6	75	90	300±30	110	90	300±30			S		18 07 29.5 ± 1.5	—20 42 15 ±45				Cwd	1	G9.9—0.7
1808—209	2		1.4	55	6.0	5.5±1.5	124	9.9	6.9±5.1			S		18 08 07.52±0.07	—20 55 43.9±1.2				Cwd	1	CC 009—01.0
1828—195	2		0.85							19	86	D	CN	18 28 05.93±0.11	—19 35 52.0±3.2				Cwd	5	
		A	0.5	61	10	≤9.5	113	8.1	≤6.5				A	18 28 05.47±0.11	—19 35 47.5±3.4						
		B	0.35	60	10	≤11	114	10	≤9.5				B	18 28 06.82±0.14	—19 35 46.1±4.1						
1831—203	2		0.45	57	15	≤10	85	7.9	≤8.1			U		18 31 37.44±0.11	—20 21 35.8±3.6				Cwd	6	
1833—192	4	S	0.85	122	4.1	≤4.2				28	35	D	CN	18 33 56.87±0.15	—19 12 41.2±2.5				Cwd	6	
		A	0.45	35	10	≤12	79	8.1	≤5.8				A	18 33 56.42±0.15	—19 12 49.2±2.0						
		B	0.4	34	10	≤12	79	15	≤21				B	18 33 57.55±0.20	—19 12 26.5±3.0						
1858—185	2		0.45	52	30	31±12	114	30	55±15			S		18 58 49.52±0.18	—18 30 45.9±4.0				Cwd	11	
1859—187	2		0.65	49	30	24±10	116	30	20±10			PD		18 59 09.62±0.20	—18 47 51.9±3.0				Cwd	11	
1905—190	2		0.8	61	30	70±10	85	30	70±10			S		19 05 18.60±0.40	—19 00 15 ±15				Cwd	12	MSH 19—101, CUL 2
*1918—185	4		1.4									Cx	CN	19 18 20.49±0.07	—18 31 46.6±1.0				EF	15	OV—130
		A	0.95	33	6.0	≤6.0	124	6.0	11.0±3.0				A	19 18 20.55±0.04	—18 31 44.4±0.7						
*1922—183	2		0.7	29	5.9	≤6.7	108	3.9	≤3.3			U		19 22 18.13±0.05	—18 19 03.6±0.9	—3.5	—4.1	19.5	RO, Cwd	16	
1933—173	5		2.0							188	42	D, Br 40%	CN	19 33 21.50±0.50	—17 18 00 ±15				INP	18	PKS
		A	0.4	38	15	≤11	59	10	≤10				A	19 33 15.70±0.35	—17 19 35 ±10						
		B	0.8	27	10	≤10	60	10	15.0±5.0				B	19 33 24.50±0.35	—17 17 15 ±10						
1938—167	4		0.85	52	15	22.0±6.0	90	30	37.0±7.0			PD		19 38 36.66±0.13	—16 42 49.0±2.5				INP	18	
1939—166	4		0.55	58	15	≤11	94	6.1	≤6.0			U		19 39 44.97±0.05	—16 37 44.2±2.4	—5.0	—0.3	18	Pair NSOs	19	OV—166.1
1940—174	2		0.4	45	30	≤20	83	30	≤19			U		19 40 44.84±0.19	—17 29 23.2±4.5				INP	19	OV—168
1945—168	2		0.8	39	20	24.0±5.0	94	15	≤12			S		19 45 54.69±0.14	—16 52 04.3±2.4				EF	20	OV—177
1959—161	2		0.7	20	6.0	6.5±2.5	121	3.0	≤2.3			S		19 59 22.44±0.07	—16 09 24.7±1.0				EF	23	
1959—159	2		0.4	66	15	≤12	72	30	≤17			U		19 59 40.97±0.67	—15 54 07 ±24				INP	23	
2000—159	3		0.4	41	15	13.0±6.5	93	10	≤9.7			S		20 00 36.32±0.06	—15 56 39.8±1.9	—0.1	—0.8	17	†NSO	23	
2001—159	2		0.35	19	10	≤11	113	20	≤27			U		20 01 11.19±0.19	—15 58 06.0±2.0				EF	23	
2013—154	2		0.4	20	10	≤11	107	3.9	≤3.1			U		20 13 28.85±0.05	—15 27 48.2±1.4				EF	26	
2014—157	2		0.85	11	4.0	≤4.0	116	4.0	≤5.0			U		20 14 13.29±0.07	—15 47 48.8±1.0				EF	26	
2019—149	4		0.25	43	29	≤24	86	60	≤80			U		20 19 27.19±0.13	—14 59 23.7±4.6				EF	27	
2023—142	2		1.0	0	3.0	2.7±1.8	141	4.0	≤2.5			S		20 23 18.70±0.10	—14 13 18.2±1.2	—6.4	—0.5	20	G	27	

TABLE 3.2 (Contd.)

(1)	(2)	(3)	(4)	(5)	(6)	(7)	(8)	(9)	(10)	(11)	(12)	(13)	(14)	(15)	(16)	(17)	(18)	(19)	(20)	(21)	(22)
2053—127	6		0.5	35	8.0	8.3±3.9	99	4.0	≤3.0			S		20 53 06.75±0.04	—12 46 17.1±1.0	+2.1	—1.4	19.5	†BG	33	OW—189
2054—123	5		0.45	25	3.0	≤3.9	101	6.0	≤4.5			U		20 54 31.90±0.06	—12 21 27.6±1.0				EF	33	
2105—119	4		1.2	15	2.9	≤2.9	99	2.0	≤2.0			U		21 05 35.61±0.02	—11 54 07.7±0.5				EF	36	
*2120—102	8		3.1	29	0.8	≤0.9	103	0.8	≤0.8			U		21 20 11.49±0.02	—10 16 08.8±0.3				EF	38	PKS
2123—103	2		0.55	27	5.9	7.1±3.4	88	4.0	≤3.6			S		21 23 02.60±0.05	—10 19 39.1±1.1				EF	39	OX—138
2127—096	2		1.3	71	15	16.5±6.5	123	9.7	10.5±6.5			PD, 3:1		21 27 17.49±0.09	—09 38 47.3±2.4	(—5	—2)	20.5	†RO	39	OX—046
2138—089	4		0.3	21	29	33 ±23	95	29	31 ±12			S		21 38 56.69±0.20	—08 56 00.8±5.0	(0	+9)	20.5	†RO, Def.?	42	
2149—084	4		0.5	19	6.0	≤5.0	98	5.9	≤5.0			U		21 49 47.09±0.05	—08 24 32.8±1.0	—0.4	—0.5	14	†EG	44	OX—083
2207—069	2		1.35	1	2.3	≤2.3	113	2.1	≤2.5			U		22 07 20.90±0.07	—06 57 29.6±1.0				EF	47	4C—06.72
2211—057	4		0.8	45	9.7	11.0±5.0	77	5.9	≤5.9			S		22 11 44.52±0.06	—05 47 15.1±2.0				EF	47	
2212—056	2		0.45	51	29	33 ±14	73	20	31 ±10			S		22 12 25.55±0.30	—05 40 25 ±10	+6.8	—11.3	15	†EG	47	
2219—053	2		0.65	28	2.9	≤3.2	89	3.9	≤4.6			U		22 19 53.91±0.05	—05 21 01.4±0.8				EF	48	OY—034
2223—053	4		1.4	16	4.0	≤2.2	50	2.0	≤2.0			U		22 23 20.39±0.04	—05 22 51.2±0.6	—0.1	—0.7	15	†EG	49	
2236—040	4		0.5	5	15	15 ±10	104	39	50±15			S		22 36 49.41±0.15	—04 01 47.5±3.0	(—2	—2)		†BO, Def.?	51	
2253—018	2		0.2	29	7.8	≤5.5	77	29	≤22			U		22 53 40.22±0.27	—01 48 49.1±2.7				EF	52	
*2304—012	2		1.15	28	2.0	≤2.7	93	2.0	<1.9			U		23 04 18.88±0.03	—01 12 47.8±0.7				EF	54	OZ—007
2308—006	2		0.45	39	5.8	≤4.5	68	7.8	≤7.2			U		23 08 53.96±0.14	—00 39 57.0±2.4				EF	54	
2320—002	2		0.3	29	5.9	≤4.5	89	15	≤12			U		23 20 04.65±0.14	—00 12 32.5±1.5				EF	55	
2322+003	2		0.45	109	9.7	20.5±4.0	178	9.7	15.5±3.5			S		23 22 14.50±0.10	+00 20 07.1±1.1	—3.5	+0.9	19	†BSO	55	
2322—000	2		0.5	55	5.9	≤4.2						U		23 22 15.60 a	—00 01 18 a				EF	56	
2322+006	2		0.75	53	5.9	≤7.0						U		23 22 25.45 a	+00 38 40 a				EF	55	
*2322+011	2		0.7	20	5.9	≤9.0	92	2.9	≤4.3			U		23 22 55.19±0.07	+01 06 05.1±1.2				EF	55	OZ 038
2323+009	2		0.3	54	7.8	≤10						U		23 23 52.85 a	+00 55 25 a				EF	55	
2333+019	2		0.55	130	8.0	≤10	172	15	≤15			U		23 33 57.23±0.30	+01 54 11.0±8.0	+2.0	+3.7	18	†QSO(4)	56	
*2342+023	2	S	0.8	106	9.8	10.5±3.5				30	16	D	CN	23 42 01.06±0.10	+02 20 01.0±3.0	—1.1	+9.8	18.5	†RG	56	OZ 071
		A	0.4	9	9.8	12.0±4.0							A	23 42 00.70±0.40	+02 19 42.6±2.0						
		B	0.4	9	7.8	10.0±5.0							B	23 42 01.27±0.40	+02 20 12.2±1.5						

(1)	(2)	(3)	(4)	(5)	(6)	(7)	(8)	(9)	(10)	(11)	(12)	(13)	(14)	(15)	(16)	(17)	(18)	(19)	(20)	(21)	(22)
2354+040	2		0.55	8	2.9	≤1.9	105	3.9	≤2.8			U	23^h	54^m 38.25±0.04	+04 01 09.5±0.6				EF	56	OZ 092
2356+033	2		1.25	44	9.8	17.0±4.0	67	7.8	11.5±3.0			S	23	56 09.04±0.13	+03 20 18.6±3.0				EF	57	4C+03.61
2359+038	2		0.45	52	3.9	≤2.9	65	7.8	<8.0			U	23	59 43.69±0.21	+03 51 26.4±4.5				EF	57	

* Additional notes in text.

† A positive or likely identification.

a Errors in Radio Position : 2322—000 : ±3″ in PA 55° and ±20″ in PA 145°
2322+006 : ±3″ in PA 53° and ±30″ in PA 143°
2323+009 : ±3″ in PA 54° and ±15″ in PA 144°

References for finding charts :—

(1) Shimmins et al. (1974)
(2) Wills et al. (1973)
(3) Bolton and Ekers (1966)
(4) Stocke and Arp (1978)

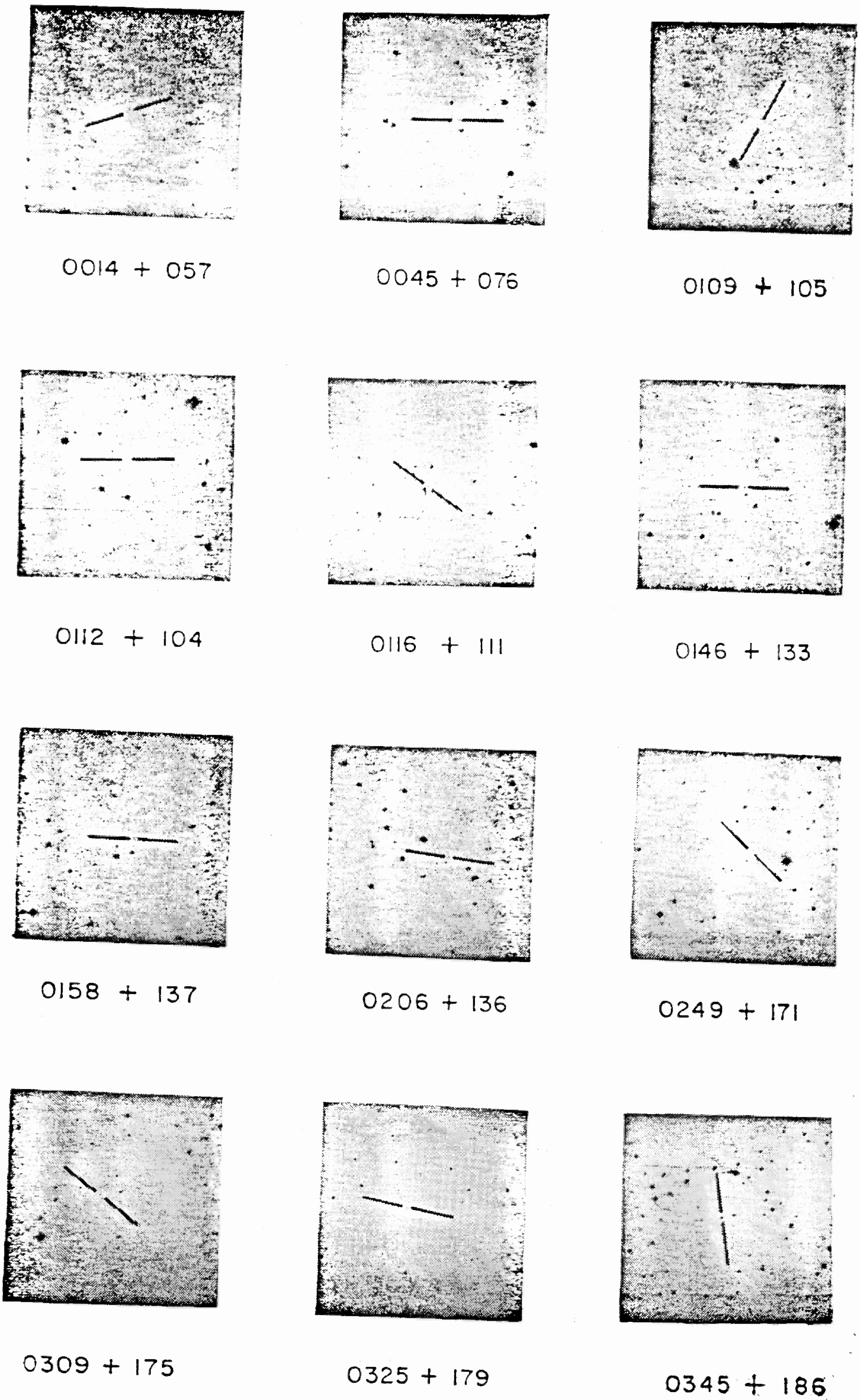

Plate 3.2: Finding charts for 54 radio sources. North is at the top and east is at the left. The field shown covers about 10 arcmin on the side.

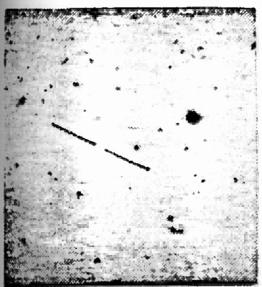

0437 + 205

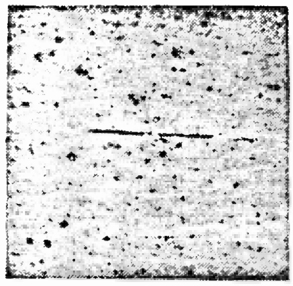

0628 + 191

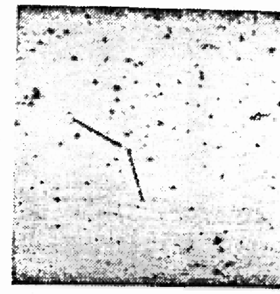

0635 + 191

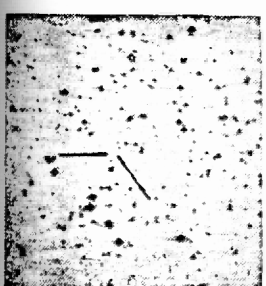

0645 + 189

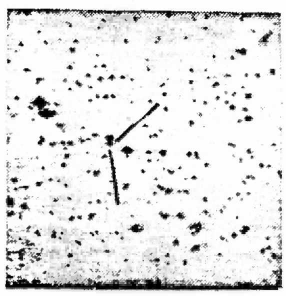

0652 + 187

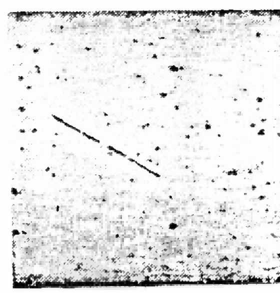

0702 + 181

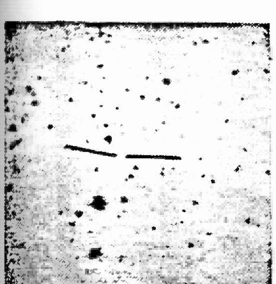

0708 + 184

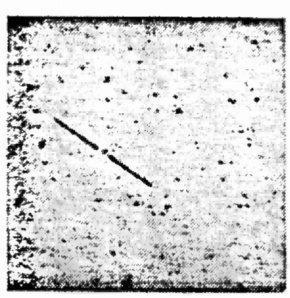

0727-+ 174

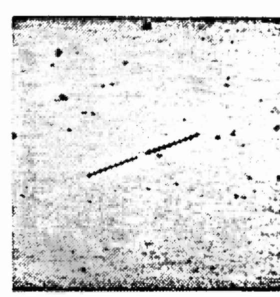

0731 + 169

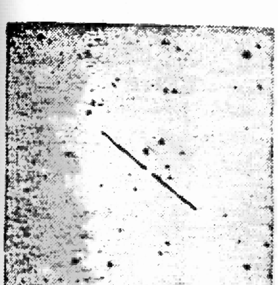

0748 + 164

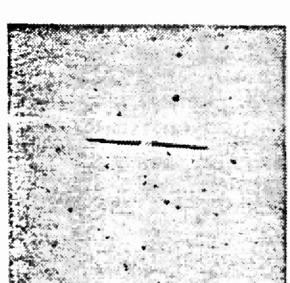

0822 + 144

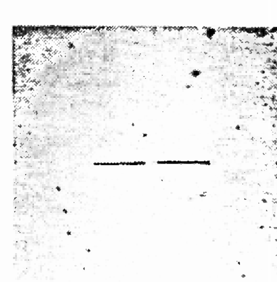

0920 + 104

Plate 3.2 (Contd.)

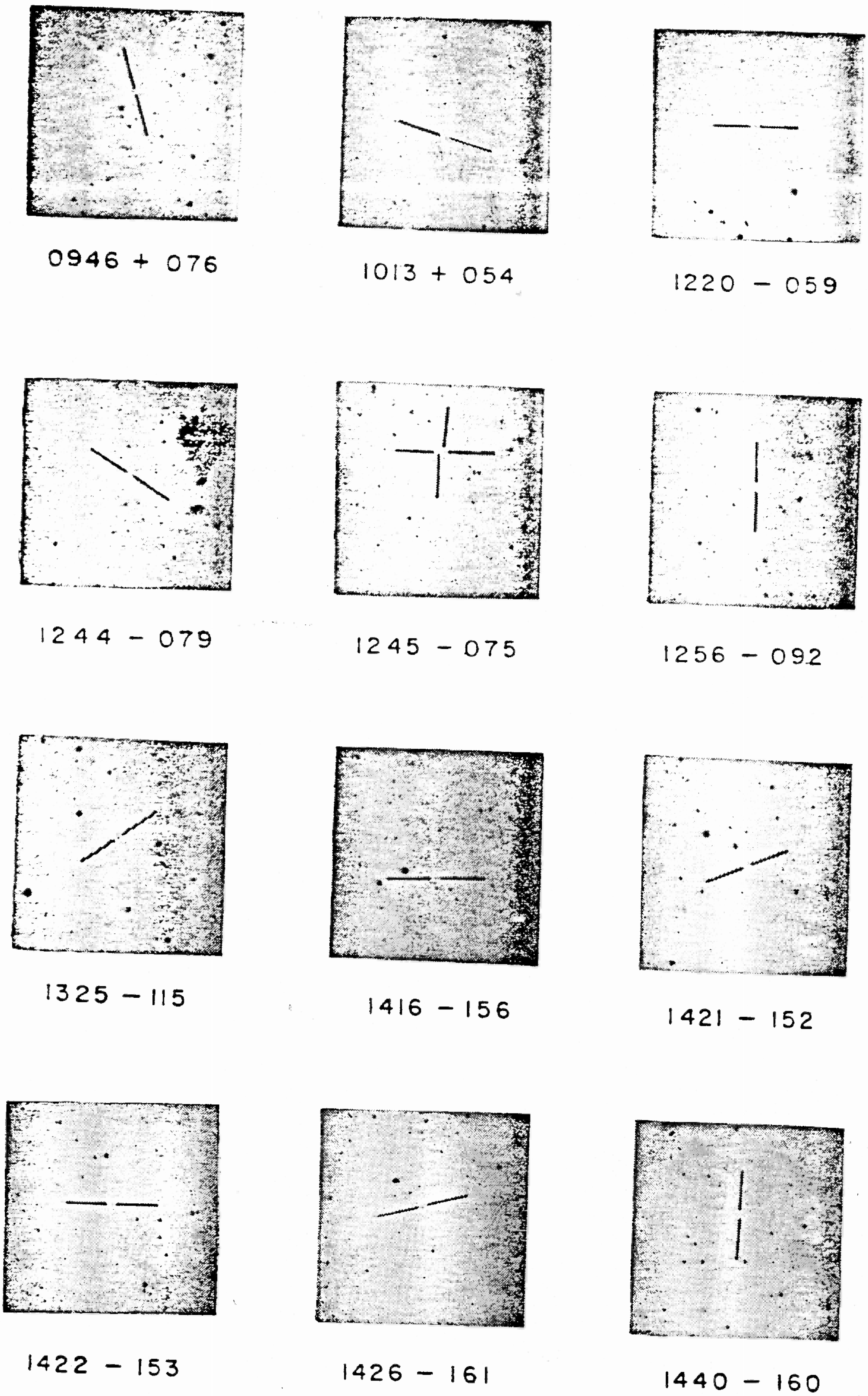

Plate 3·2 (Contd.)

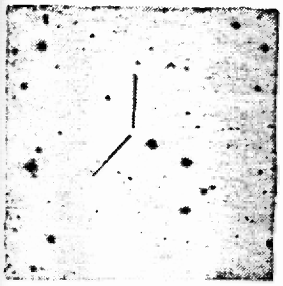

1445 − 161

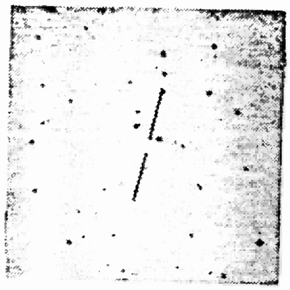

1452 − 168

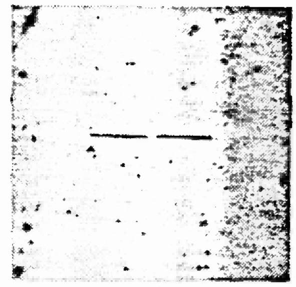

1456 − 165

1522 − 188

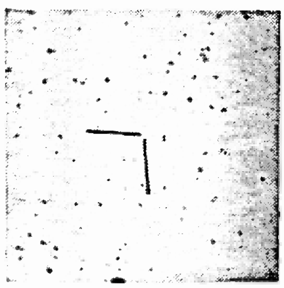

1524 − 181

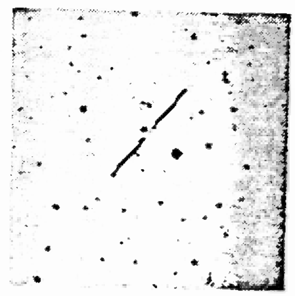

1531 − 182

1631 − 201

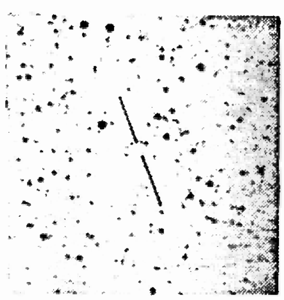

1655 − 201

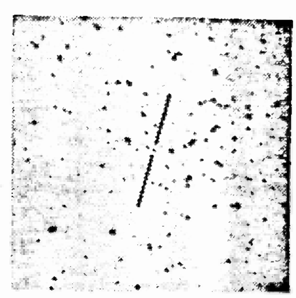

2000 − 159

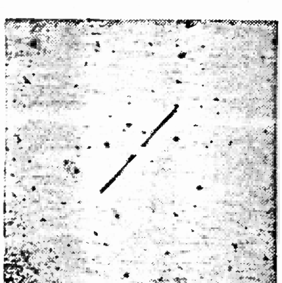

2053 − 127

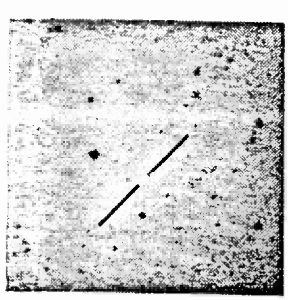

2127 − 096

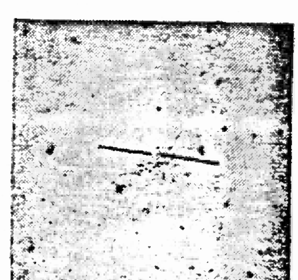

2138 − 089

Plate 3.2 (Contd.)

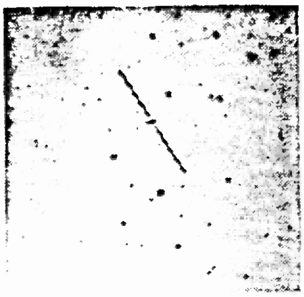

2149 − 084

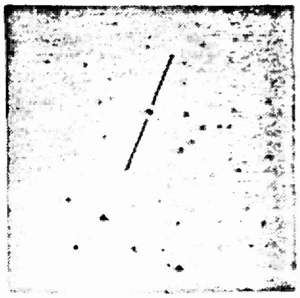

2212 − 056

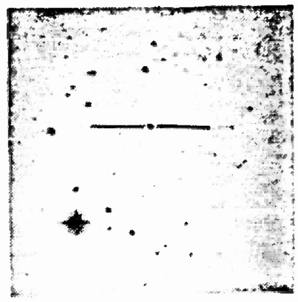

2223 − 053

2236 − 040

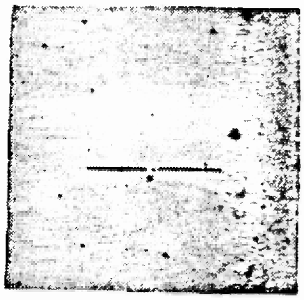

2322 + 003

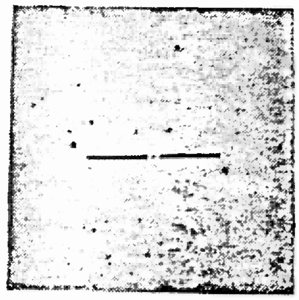

2342 + 023

Plate 3.2 (Contd.)